FLOW IN CURVED CHANNELS

A REVIEW OF THE PRESENT KNOWLEDGE

RMD Report L-32

Alberta
ENVIRONMENT
Research Management Division

RESEARCH MANAGEMENT DIVISION LOGO

The logo represents the interdisciplinary and holistic nature of the Division's environmental research programs. Each of the five sections of the symbol represent comprehensive programs on air, water, land, humans and their constant interaction. The sections converge to form a cohesive chain, characteristic of an effective research organization. This cohesive bonding makes the sections blossom into the environment in the form of a flower — an Albertan wild rose.

FLOW IN CURVED CHANNELS

A REVIEW OF THE PRESENT KNOWLEDGE

RMD Report L-82

April 1983

For information on reports published by the Research Management Division, contact:

Research Management Division
14th Floor, Standard Life Centre
10405 - Jasper Avenue
Edmonton, Alberta
T5J 3N4

(403) 427-3943

This report may be cited as:

Steffler, P.M., N. Rajaratnam, and A.W. Peterson. 1993. Flow in curved channels: A review of the present knowledge. Prep. for the Research Management Division, Alberta Environment by the Department of Civil Engineering, University of Alberta. RMD Report L-82. 60 pp.

FLOW IN CURVED CHANNELS

A REVIEW OF THE PRESENT KNOWLEDGE

by

P.M. STEFFLER
N. RAJARATNAM
A.W. PETERSON

Department of Civil Engineering
University of Alberta

for

Research Management Division
Alberta Environment

RMD Report L-82

April 1983

This report is made available as a public service. The Alberta Department of Environment neither approves nor disagrees with the conclusions expressed herein, which are the responsibility of the authors.

TABLE OF CONTENTS

		Page
LIST OF TABLES		vii
LIST OF FIGURES		viii
ABSTRACT		ix
ACKNOWLEDGEMENTS		x
1.	INTRODUCTION	1
2.	MECHANICS OF CURVED CHANNEL FLOW	2
2.1	Introduction	2
2.1.1	Co-ordinate System	2
2.1.2	General Assumptions	4
2.2	Superelevation	4
2.2.1	Derivation	5
2.2.2	Superelevation Example	7
2.2.3	Effect of Varying Longitudinal Velocity	8
2.2.4	Effect Of Bed Friction	9
2.2.5	Calculation of Superelevation	12
2.2.6	Developing Flow Considerations	13
2.3	Secondary Flow	14
2.3.1	Analysis of Developed Secondary Flow in a Wide Open Channel	14
2.3.2	Bank Effects	19
2.3.3	Developing Secondary Flow	19
2.4	Longitudinal Velocity Redistribution	21
2.4.1	Inertial Effects	23
2.4.2	Slope Differential Effect	25
2.4.3	Depth of Flow (Vertical Friction)	27
2.4.4	Lateral Friction	27
2.4.5	Lateral Momentum Transport by Secondary Flow	28
2.4.6	Developing Flow	29
2.5	Bed Shear Stress	30
2.6	Wall Shear Stress	32
2.7	Friction Coefficent	32
2.8	Bed Scour and Topography	33
2.8.1	Developed Bed Profile	33
3.	REVIEW OF EXPERIMENTAL INVESTIGATIONS	39
3.1	Fixed Boundary Channels	39
3.2	Mobile Boundary Channels	46
3.3	Natural Stream Observations	46
4.	MATHEMATICAL MODELS	47
4.1	Three-Dimensional Models	47
4.2	Two-Dimensional Model	48
4.3	One-Dimensional Models	49
4.4	Summary	49
5.	CONCLUSIONS	50
5.1	Mechanics of Flow in Curved Channels	50
5.2	Experimental Studies	50
5.3	Mathematical Models	51
6.	REFERENCES CITED	52

7. APPENDIX - PROGRAM CRVCNL 55
7.1 Input to CRVCNL 55
7.2 Output 56
7.3 Program Example 56

LIST OF TABLES

Page

1. Rigid Boundary Curved Channel Experiments 40
2. Mobile Boundary Curved Channel Experiments 44
3. Natural Stream Bend Measurements 45

LIST OF FIGURES

		Page
1.	Definition Sketch – Plan	3
2.	Definition Sketch – Elevation	3
3.	Forces Acting on a Water Column	6
4.	Superelevation Versus Curvature Ratio	10
5.	Secondary Circulation	15
6.	Integral Functions	20
7.	Redistribution of Longitudinal Velocity	22
8.	Slope Differential	26
9.	Bed Shear Stress Distribution	31
10.	Particle Equilibrium	34
11.	Maximum Scour Versus Curvature Ratio	37
12.	Input for Program Example	57
13.	Output From Program Example	58
14.	Program Listing	59

ABSTRACT

Curvature affects the flow of water in open channels in several ways. These effects include superelevation, secondary (induced) flows, longitudinal velocity redistribution, and bed scour in the case of a mobile boundary such as a natural stream or river. It is important for river engineers to understand and be able to estimate these effects.

This report presents and discusses the present state of knowledge and understanding of the problem of curved channel flow. The flow mechanics are discussed first with an emphasis on the prediction of specific flow phenomena. The state of the art is found to be adequate with regard to some effects but not others. A body of experimental data obtained under controlled conditions is an important component of the state of knowledge of a field. The existing curved channel experiments are tabulated and evaluated in the second part of this report. Finally, a discussion of the relatively recent application of numerical modelling is presented. Aspects of the problem requiring further research and elaboration are identified in the conclusions of this report.

ACKNOWLEDGEMENTS

The authors wish to acknowledge the efforts of D.T. Sneddon, M.E. Quazi, and G.D. Fonstad during the initiation and review phases of this report. This project was funded by a grant from the Research Management Division, Alberta Environment.

1. INTRODUCTION

Almost all rivers and streams are curved or meandering to some degree. This curvature has a considerable effect on the flow, bed topography, and dispersion characteristics of the stream. Usually, in practical situations, designers avoid curved reaches or take account of these effects with simple but overconservative estimates. It is the purpose of the present report to analyse the state-of-the-art knowledge of curved channel flows and to obtain estimates of these effects such that they may be used in hydraulic engineering practice.

Generally, the state of present knowledge may be divided into the following three areas:

1. The flow mechanics which form the basis of our understanding of the problem.
2. A body of experimental information which provides validation of theories and guidelines for practical situations.
3. Predictive models which may be used for detailed design and analysis.

Each of these will be considered separately.

2. MECHANICS OF CURVED CHANNEL FLOW

2.1 INTRODUCTION

In order to make engineering judgements and calculations, a reasonable understanding of the physics of the problem is required. At the present time, some aspects of flow in curved open channels are well understood while others are not. The present section will attempt to explain the features of curved channel flow in an engineering manner; that is, to provide qualitative descriptions which are backed up with straightforward formula derivations and pertinent experimental results.

2.1.1 Co-ordinate System

The co-ordinate system used will be based on Figure 1, where x and u are the longitudinal direction and velocity, y and v are the lateral direction and velocity, while z and w are the vertical direction and velocity. The radius of curvature of the channel centreline is R_0 and the width and average depth of the channel are given by B and H_0 respectively.

The radius of curvature of any point across the channel is given by r which is related to R_0 and y:

$$r = R_0 + y \tag{1}$$

h is the elevation of the water surface above H_0 (referring to Figure 2) while H_S is the scour depth below the mean bed elevation. The actual depth of flow is represented by d and is given by:

$$d = H_0 + H_S + h \tag{2}$$

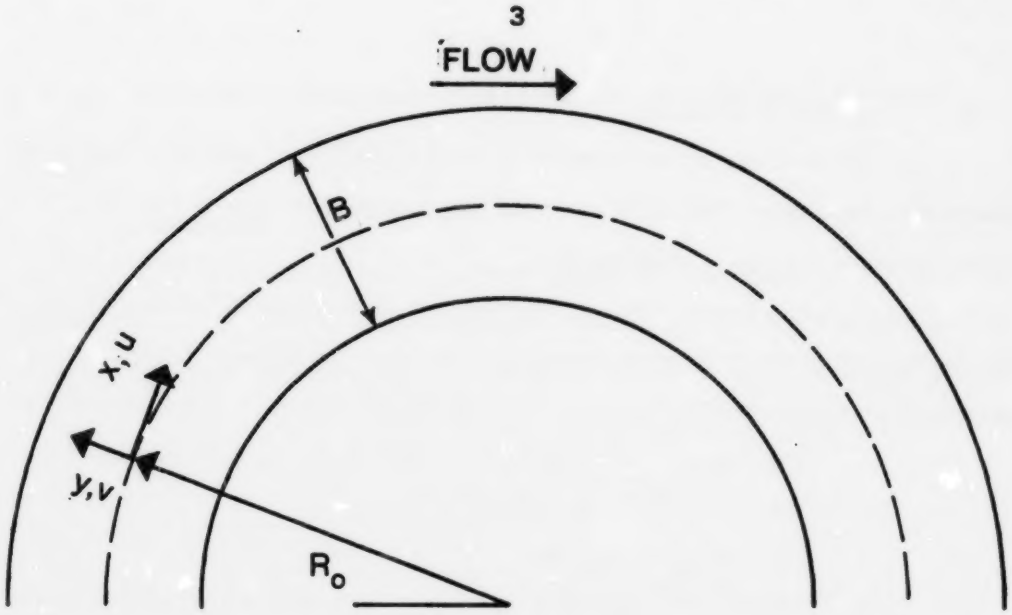

Figure 1. Definition Sketch - Plan

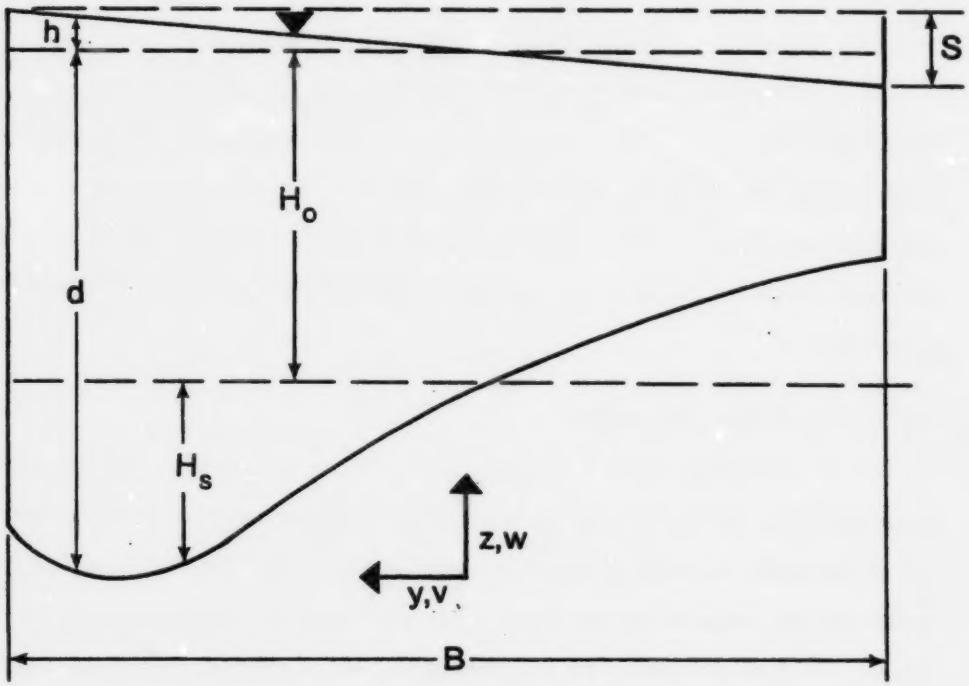

Figure 2. Definition Sketch - Elevation

2.1.2 General Assumptions

All velocities are assumed to be time averaged and the flow itself is assumed to be steady. The depth averaged longitudinal velocity is U and the cross-sectional average is given by U_s.

In much of what follows, the flow will be assumed to be "developed", that is, invariant in the longitudinal direction. This condition has also been described as "axisymmetric". The requirements for developed flow are as follows:

1. The radius of curvature of the channel (R_s) remains constant (i.e., the bend is circular in plan).
2. The channel is prismatic.
3. The section under consideration is well removed from the entrance and exit. (i.e., the bend is long).

These conditions are quite restrictive and are rarely met in a laboratory, much less in the field. The developed flow assumption is useful, however, in isolating some features of the flow for better understanding.

The procedure in the following will be to attack the individual phenomena separately. This results in the simplest presentation, but it must be remembered that there are significant interactions between them and a proper approach would be to find a solution for the flow as a whole. The relative depth of presentation of the different aspects is indicative of the state-of-the-art understanding.

2.2 SUPERELEVATION

The most obvious consequence of flow around a curved channel is superelevation, that is, the rise of the water surface around the outside, and the fall of the water surface around the inside of the bend. The magnitude of this water surface slope is not large but it has important indirect consequences.

The explanation of this phenomena is, of course, centrifugal force. That is, for the water to follow a circular path, a force must be applied in a direction normal to the flow and directed toward the centre of curvature. This is

provided by the excess hydrostatic pressure of an increased depth of water towards the outside of the bend.

2.2.1 Derivation

To calculate the water surface profile, consider Figure 3, a free body diagram of a water column of thickness Δx, flowing concentrically around a bend with depth averaged velocity U. The balance of forces acting on this fluid element is:

$$\frac{mU^2}{r} - (P_o - P_1) - F = 0 \qquad (3)$$

where P_o and P_1 are hydrostatic pressure forces and F is lateral bed shear force. m is the mass of the element:

$$m = \frac{\gamma}{g} d\Delta r \qquad (4)$$

where γ is unit weight of the fluid and g is the acceleration due to gravity. Substituting 4 and the hydrostatic forces into 3 we have:

$$\frac{U^2}{r} \frac{\gamma}{g} d\Delta r - \left(\frac{\gamma}{2}\left(d+\frac{\Delta h}{2}\right)^2 - \frac{\gamma}{2}\left(d-\frac{\Delta h}{2}\right)^2\right) - F = 0 \qquad (5)$$

Simplifying and ignoring terms of order (h^2):

$$\frac{U^2}{r} \frac{\gamma}{g} d\Delta r - \gamma d\Delta h - F = 0 \qquad (6)$$

or:

$$\frac{\Delta h}{\Delta r} = \frac{U^2}{gr} - \frac{F}{\gamma d\Delta r} \qquad (7)$$

or in the limit as $r \rightarrow 0$:

$$\frac{dh}{dr} = \frac{U^2}{gr} - \frac{\tau_{y0}}{d\gamma} \qquad (8)$$

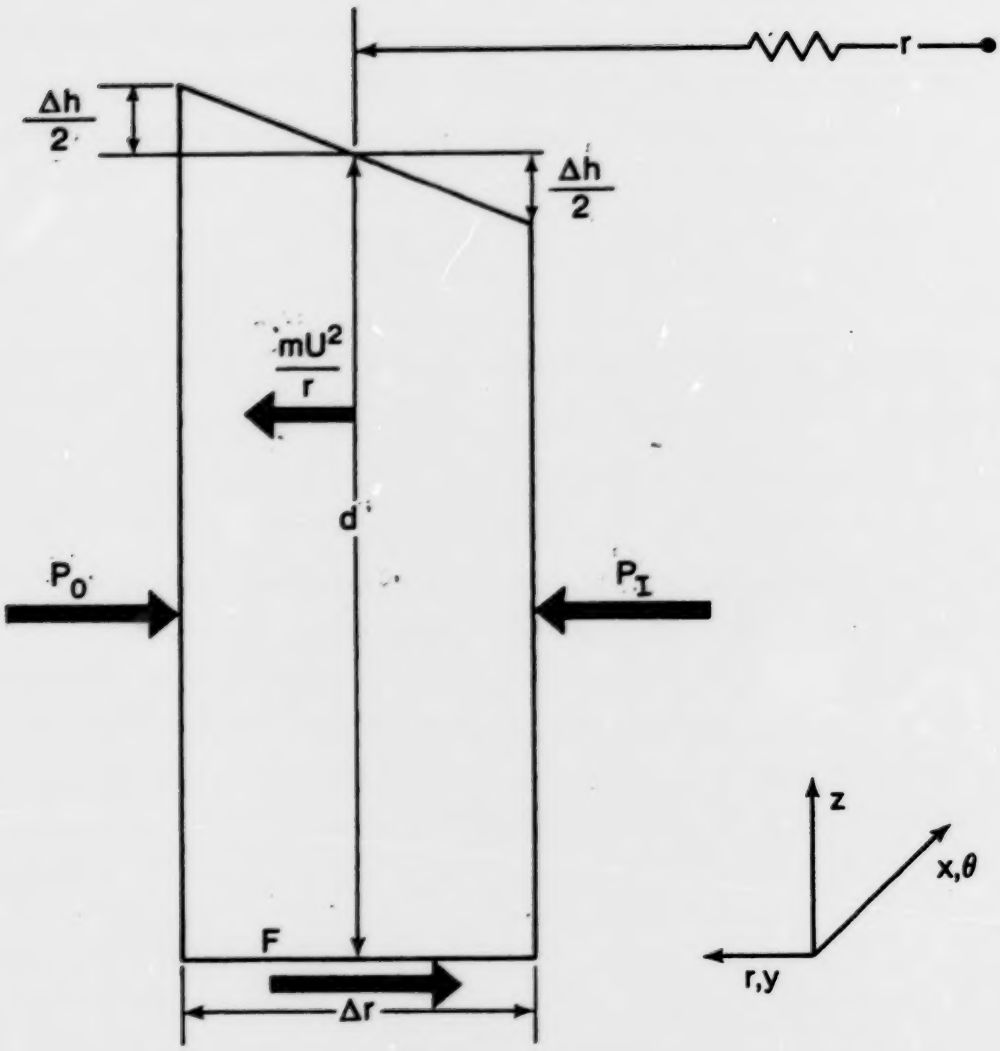

Figure 3. Forces acting on Water Column

where τ_{y0} is the bed shear stress in the lateral direction. In many cases, it is small and may be neglected. As a first approximation we may take U equal to U_s and r equal to R_s such that:

$$\frac{dh}{dr} = \frac{U_0^2}{gr} \tag{9}$$

Equation 9 may be integrated by noting from 1:

$$dr = dy \tag{10}$$

to give:

$$h = \frac{U_0^2}{gR_0} y \tag{11}$$

At the outside of the bend:

$$h = \frac{U_0^2}{2g} \frac{B}{R_0} \tag{12}$$

and the total superelevation (difference between outside and inside elevations) is:

$$S = 2 \frac{B}{R_0} \frac{U_0^2}{2g} \tag{13}$$

2.2.2 Superelevation Example

As an example to illustrate the size of this superelevation, take the North Saskatchewan River bend around the Mayfair golf course in Edmonton (data from Kellerhalls et al. 1972), where:

$$B = 140 \text{ m} \tag{14}$$

$$U_0 = 1.25 \text{ m/s} \tag{15}$$

$$S = 30 \text{ mm} \tag{16}$$

Thus:

$$R_0 = 750 \text{ m} \tag{17}$$

This does not seem large, considering that this particular bend is of only moderate curvature , but the cross channel slope:

$$\frac{S}{B} = 0.00021 \tag{18}$$

is of the same order of magnitude as the longitudinal bed slope:

$$S_0 = 0.00035 \tag{19}$$

The above estimation of superelevation has been found experimentally to be accurate to within about ten percent, although it consistently underestimates the superelevation. In some cases of erodable bed laboratory models, superelevations of up to twice this value have been observed (Yen and Yen 1971).

2.2.3 Effect of Varying Longitudinal Velocity

To improve this estimate, one approach taken is to allow U to vary across the channel. The problem, then, is to specify the variation of U. Ippen and Drinker (1962) tried several variations:

$$\text{a. the free vortex; } U = U_0 \frac{R_0}{r} \tag{20}$$

Just past the entrance of the bend, the velocity will be distributed according to equation 20. The corresponding expression for superelevation was derived to be:

$$S = 2 \frac{B}{R_0} \frac{U_0^2}{2g} \left(\frac{1}{1 - \left(\frac{B}{2R_0}\right)^2} \right) \tag{21}$$

b. the forced vortex; $U = U_0 \frac{r}{R_0}$ (22)

The "forced vortex" distribution approximates the flow near the end of the bend where the maximum velocity has shifted to the outside. The superelevation is then:

$$S = 2 \frac{B}{R_0} \frac{U_0^2}{2g} \left(\frac{1}{1 + \frac{1}{3} \left(\frac{B}{2R_0} \right)^2} \right) \quad (23)$$

Another possibility is to allow r to remain variable. This results (assuming $U = U_0$ again) in:

$$S = 2 \frac{U_0^2}{2g} \left(\ln \left(\frac{1 + \frac{B}{2R_0}}{1 - \frac{B}{2R_0}} \right) \right) \quad (24)$$

Figure 4 is a plot of Equations 19, 21, 23, and 24. The different formulas diverge widely for large values of B/R_0, but at values typical of natural streams ($B/R_0 < 0.5$) the difference is very small. The free vortex form, equation 21, is generally prefered since it predicts a superelevation slightly larger than the simple expression, Equation 19. The actual cross channel profile is also best fitted by the free vortex form (Ippen and Drinker 1962; Yen and Yen 1965; Yen 1971).

2.2.4 Effect Of Bed Friction

It remains, however, to consider the effect of the bed friction on the superelevation . This bed friction acts as a result of the secondary circulation which is to be considered later. For now, we will borrow two significant results that will allow us to estimate a correction to the superelevation.

First, the secondary flow near the bed is always towards the inside of the bend. This imples that the bed shear force acts in a negative sense according to the arrow on Figure 3. Thus, from Equation 8, the lateral water surface slope is always effectively increased by the bed friction.

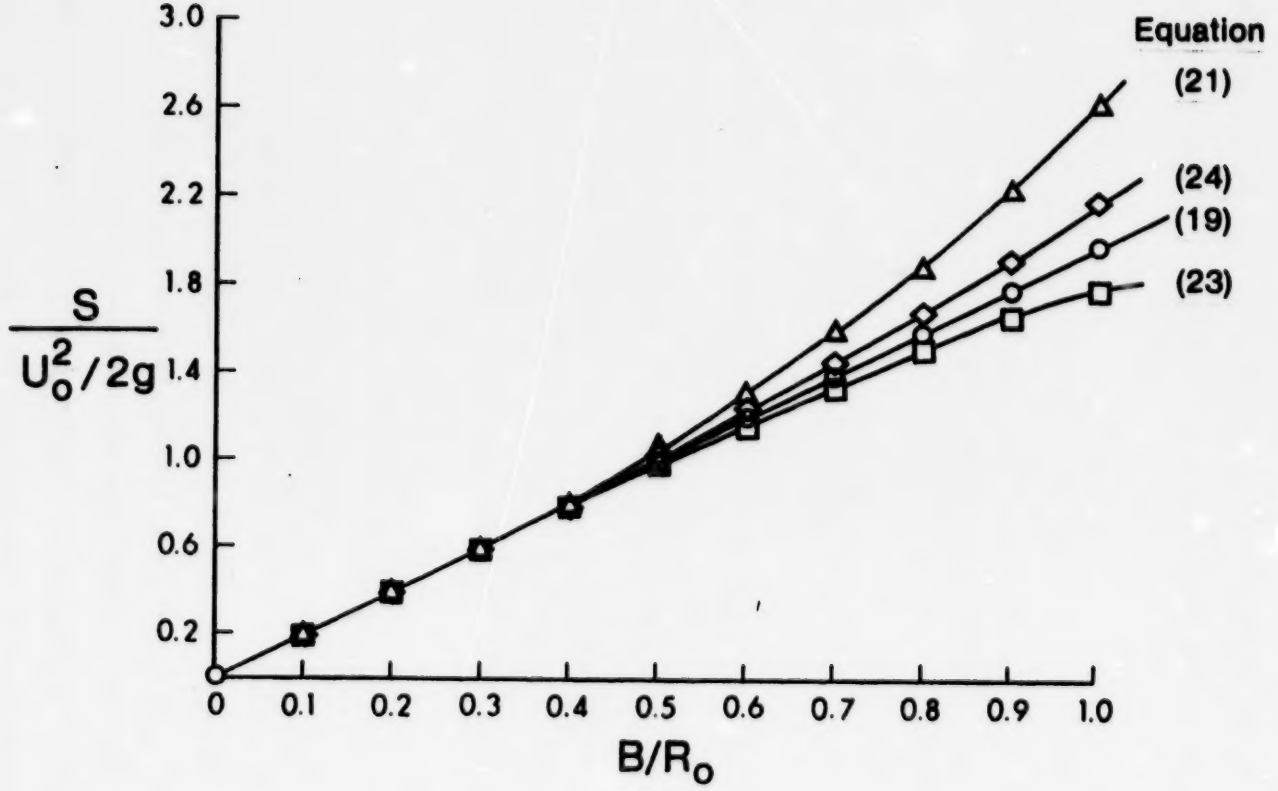

Figure 4. Superelevation vs. Curvature Ratio

To estimate the size of the correction let

$$\tau_{y0} = \tau_{x0} \tan\delta \tag{25}$$

where τ_{x0} is longitudinal bed stress and δ is the angle of the total bed stress vector from the longitudinal direction. Also define:

$$\tau_{x0} = -(\gamma/g)\ u_+^2 \tag{26}$$

where u_+ is the friction velocity and:

$$C_+^2 = U^2/u_+^2 \tag{27}$$

where C_+ is a nondimensional Chezy coefficient:

$$C_+ = C/\sqrt{g} \tag{28}$$

Substitute the above into Equation 8:

$$\frac{dh}{dr} = \frac{U^2}{gr} + \frac{U^2}{g}\frac{\tan\delta}{C_+^2 d} \tag{29}$$

Now make use of the second result to be obtained later, namely:

$$\tan\delta = 11\ \frac{d}{r} \tag{30}$$

Equation 29 becomes:

$$\frac{dh}{dr} = \frac{U^2}{gr}\left(1 + \frac{11}{C_+^2}\right) \tag{31}$$

Since typical values of C_+ range from about 10 (rough) to 20 (smooth), the correction is about 2.5% to 10% and accounts for some of the observed error. This correction applied to any of Equations 19 to 24 will result only in the magnification of the curves by the factor $(1+11/C_+^2)$. In practice it is difficult to

apply this correction because the constant, taken above as 11, actually is a function of C_+ itself and has been quoted as varying from about 7 to 13 (Koch 1980).

2.2.5 Calculation of Superelevation

In practical river situations where it is of interest the superelevation may be calculated by the following method:

1. Obtain the average stage elevation for the desired discharge by standard methods.
2. Obtain a cross-sectional bed profile of the channel (which should be measured but may be estimated using the results of section 2.6). Variations of the resistance coefficent across the channel (e.g., flood plains) should be noted as well.
3. Calculate U at a number of evenly spaced locations across the channel. At present, the best estimate is given by a resistance equation, such as:

$$U = C_+ \sqrt{gdS_0} \tag{32}$$

Note that the local resistance coefficent may require a minor adjustment to give the same discharge as specified.

4. Integrate Equation 24 numerically across the channel starting at the inside bank. Use the values of U, r (measured from the centre of curvature) and C_+ estimated previously at each point. This gives the water surface profile relative to the elevation at the inside bank.
5. The constant of integration is determined by calculating the average elevation increase of the profile from step 4. This value is subtracted from the water surface elevations to give h(y).
6. It may be necessary to repeat the process (starting at step 3) once using the new water surface elevations.

2.2.6 Developing Flow Considerations

For the case of developing flow, little is known. At a sudden change in curvature, such as at the beginning or exit of a circular bend, the water surface slope has been noticed to adjust over a length about equal to the width of the stream.

$$L_B \approx B \tag{33}$$

and roughly symmetrical on each side of the point of curvature change. Over a long bend, the magnitude of superelevation decreases slightly as the flow distribution maximum shifts from the inside to the outside of the bend. This corresponds to a gradual shift of superelevation given by Equation 21 to a value given by Equation 23.

The lateral inertia of the flow may also have a significant effect on the transverse water surface profile. Yen and Yen (1971) and Kalkwijk and deVriend (1980) both noticed a large increase in superelevation (up to twice the normal value) in experiments performed in channels with a rigid but "natural" bed. That is, there was a scour hole effect. Both experimenters attributed this effect mainly to lateral inertia. The mechanism is essentially as follows. As the flow proceeds into the bend, it encounters the scour hole on the outside of the bend. Here the flow is faster and, therefore, a large portion of the discharge shifts to the outside. This shifting entails considerable inertia and, in order to stop the lateral flow, an extra transverse water surface slope is set up.

This effect has been taken into account only in the very complex numerical models (Leschziner and Rodi (1979), deVriend 1981). As it is expected that in some cases the effect is significant, especially in natural channels, more research and application is required.

2.3 SECONDARY FLOW

Secondary circulation, or helicoidal flow as it is sometimes called, arises from the fact that some of the fluid, specifically near the bed, is moving slower than the average velocity. Since it is moving slower, it lacks the apparent centrifugal force to resist the imposed pressure gradient of the water surface slope. It is, therefore, accelerated inward until friction provides a balancing force. Fluid moving faster than average (near the surface) would experience the opposite effect and be accelerated outward. The net result is a circulation over the flow cross-section, superimposed on the main longitudinal flow (Figure 5) . The total streamlines follow a helicoidal path.

The secondary flow is important because it is believed to be the primary cause of river bend scour. It also has significant effects on the lateral diffusion characteristics of a stream.

2.3.1 Analysis of Developed Secondary Flow in a Wide Open Channel

The lateral force balance equation for an element of fluid is:

$$-\frac{u^2}{r} = -\frac{\partial(gh)}{\partial r} + \frac{\partial \tau_{yz}}{\partial z}\frac{g}{\gamma} \tag{34}$$

where τ_{yz} is the lateral shear stress acting on the top and bottom faces of the element. Equation 34 has been derived and used by Rosovskii (1961), Yen (1965), and Engelund (1974). It is directly analagous to Equation 8 except that it has been derived for a fluid element of depth dz instead of for a column of depth equal to the depth of flow d. Alternatively, Equation 34 may be derived from the Reynold's Equation for the radial direction by neglecting the inertial terms and the small stress terms.

To proceed, substitute Equation 8 into Equation 34 (noting that h is not a function of z so the partial derivative may be replaced by an ordinary derivative):

$$-\frac{u^2}{r} = -\frac{\overline{u^2}}{r} + \frac{g}{\gamma}\frac{\tau_{y0}}{d} + \frac{\partial \tau_{yz}}{\partial z}\frac{g}{\gamma} \tag{35}$$

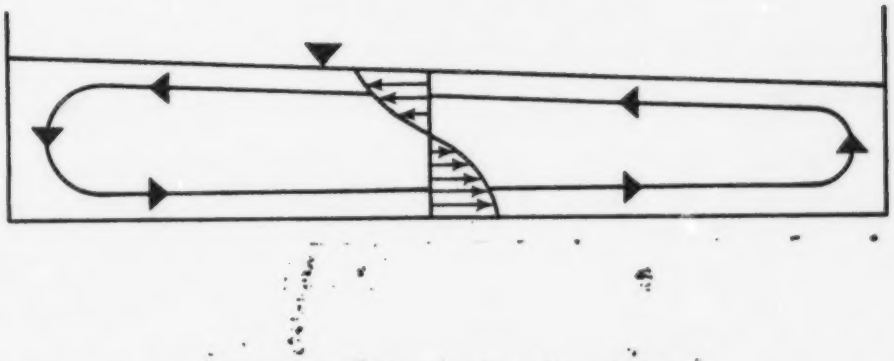

Figure 5 Secondary Circulation

A small change has been introduced into Equation 8. The term u^2, defined by:

$$\overline{u^2} = \frac{1}{d} \int_0^d u^2 dy \tag{36}$$

(which is the average over the depth of the longitudinal velocity squared) has replaced the average velocity squared, U^2, which is given by:

$$U^2 = \left(\frac{1}{d} \int_0^d u \, dy\right)^2 \tag{37}$$

The difference between the two is small, but the former is more correct.

Rearranging 35:

$$\frac{g}{\gamma} \frac{\partial \tau_{yz}}{\partial z} = \frac{1}{r} (\overline{u^2} - u^2) - \frac{g}{\gamma} \frac{\tau_{y0}}{d} \tag{38}$$

Let:

$$u = U + u' \tag{39}$$

where U is the depth average velocity and u' is the deviation from the average.

Substitute into 38:

$$\frac{g}{\gamma} \frac{\partial \tau_{yz}}{\partial z} = \frac{1}{r} (U^2 + 2 \overline{Uu'} + \overline{u'^2} - U^2 - 2Uu' - u'^2) - \frac{g}{\gamma} \frac{\tau_{y0}}{d} \tag{40}$$

Simplify Equation 40 to obtain:

$$\frac{g}{\gamma} \frac{\partial \tau_{yz}}{\partial z} = \frac{1}{r} (-2Uu' - u'^2 + \overline{u'^2}) - \frac{g}{\gamma} \frac{\tau_{y0}}{d} \tag{41}$$

To proceed further let:

$$\frac{g}{\gamma} \tau_{yz} = \varepsilon \frac{\partial v}{\partial z} \tag{42}$$

where ε is the eddy viscosity and may be a function of z. Also let:

$$\frac{g}{\gamma} \tau_{y0} = -u_*^2 \tan\delta \tag{43}$$

where δ is as defined previously. Assume:

$$u' = u_* f_1 \left(\frac{z}{d}\right) \tag{44}$$

$$\varepsilon = u_* d \, f_2 \left(\frac{z}{d}\right) \tag{45}$$

$$\eta = z/d \tag{46}$$

Substitute 42 to 46 into 41:

$$\frac{\partial}{\partial \eta} f_2 \frac{\partial v}{\partial \eta} = \frac{Ud}{r} \left(-2f_1 - \frac{1}{C_*} \left(f_1^2 - \overline{f_1^2} - \frac{r}{d} \tan\delta\right)\right) \tag{47}$$

Integrate twice with respect to η to obtain:

$$v = \frac{Ud}{r} \int \frac{1}{f_2} \left[\int \left\{-2f_1 - \frac{1}{C_*}\left(f_1^2 - \overline{f_1^2} - \frac{r}{d}\tan\delta\right)\right\} d\eta + c_1\right] d\eta + C_2 \tag{48}$$

The constants of integration are determined by:

$$f_2 \frac{\partial v}{\partial \eta} = 0 \quad \text{at} \quad \eta = 1 \tag{49}$$

(shear stress equals zero at water surface) and:

$$\int_0^1 v \, d\eta = 0 \tag{50}$$

(net lateral discharge equals zero). It remains to evaluate tan δ. This term is clearly of small magnitude as it amounts to a small correction to the lateral water surface slope. Yen (1965) and Rosovskii (1961) ignore it for certain cases. It may be evaluated by application of another boundary condition at the bed. The most obvious is simply:

$$v\big|_{\eta = 0} = 0 \tag{51}$$

de Vriend (1976) modified this condition slightly to use with logarithimic velocity distributions and stated:

$$v|_{\eta = \eta_0} = 0 \tag{52}$$

where η_0 is the height where the longitudinal velocity given by the logarithimic formula vanishes.

Another possible bed condition is that the angle of the shear stress vector at the bed should coincide with the angle of the velocity vector near the bed:

$$\frac{v}{u} = \frac{\tau_{y0}}{\tau_{x0}} = \tan\delta = \frac{\varepsilon \, \partial v/\partial y}{u_+^2} \tag{53}$$

A difficulty with this condition is that the level of the velocity vector must be specified. Rosovskii (1961) and Engelund (1974) used this condition. De Vriend (1976) reviews these conditions.

In general the results take the form:

$$\tan\delta = K \frac{d}{r} \tag{54}$$

where K is a fuction of C_+ and of the particular velocity and eddy viscosity distributions. Values of K ranging from 7 to 13 have been reported, with K = 11 a reasonable approximation for typical stream conditions (Koch 1980; Rosovskii 1961). Equation 54 may be substituted into Equation 48 which may be written as:

$$v = \frac{Ud}{r} \left[I_1 + \frac{I_2}{C_+} \right] \tag{55}$$

where:

$$I_1(\eta) = \int \frac{1}{f_2} \left(\int -2 f_1 d_\eta + a_1 \right) d\eta + a_2 \tag{56}$$

$$I_2(\eta) = \int \frac{1}{f_2} \left(\int \{ -f_1^2 + \overline{f_1^2} + K \} \, d\eta + b_1 \right) d\eta + b_2 \qquad (57)$$

The problem is thus solved when the distributions f_1 and f_2 are supplied. Figure 6 is a graph of I_1 and I_2 when the logarithimic distribution of u is chosen for f_1 and a parabolic distribution of eddy viscosity is chosen for f_2. K is assumed to equal 11. Von Karman's constant is taken as 0.4.

In general, increasing roughness (decreasing C_+) leads to smaller secondary velocities, especially near the bed.

2.3.2 Bank Effects

At the stream banks, the lateral flow is turned vertically to complete the secondary circulation. At the outside bank, the flow is downward while at the inside bank it is upward. Calculations have been made for this region (Rosovskii 1961; de Vriend 1973) and some useful conclusions have been obtained (for rectangular channels at least):

1. Wall effects (that is, appreciable vertical velocity) extend about twice the flow depth into the channel from the banks.
2. The maximum vertical velocities are about the same as the maximum lateral velocities in the centre of the channel.

For other than rectangular channels, information is scarce.

2.3.3 Developing Secondary Flow

As the fluid possesses inertia, there is a certain length required to set the secondary circulation into motion after the bend entrance. If we assume that the water surface changes abruptly from flat to superelevated, then the development length, or distance to reach 90% of its developed value, has been estimated to be (Rosovskii 1961; Nouh and Townsend 1979):

$$L_s = (1.8 \text{ to } 2.3) \, H_0 \, C_+ \qquad (58)$$

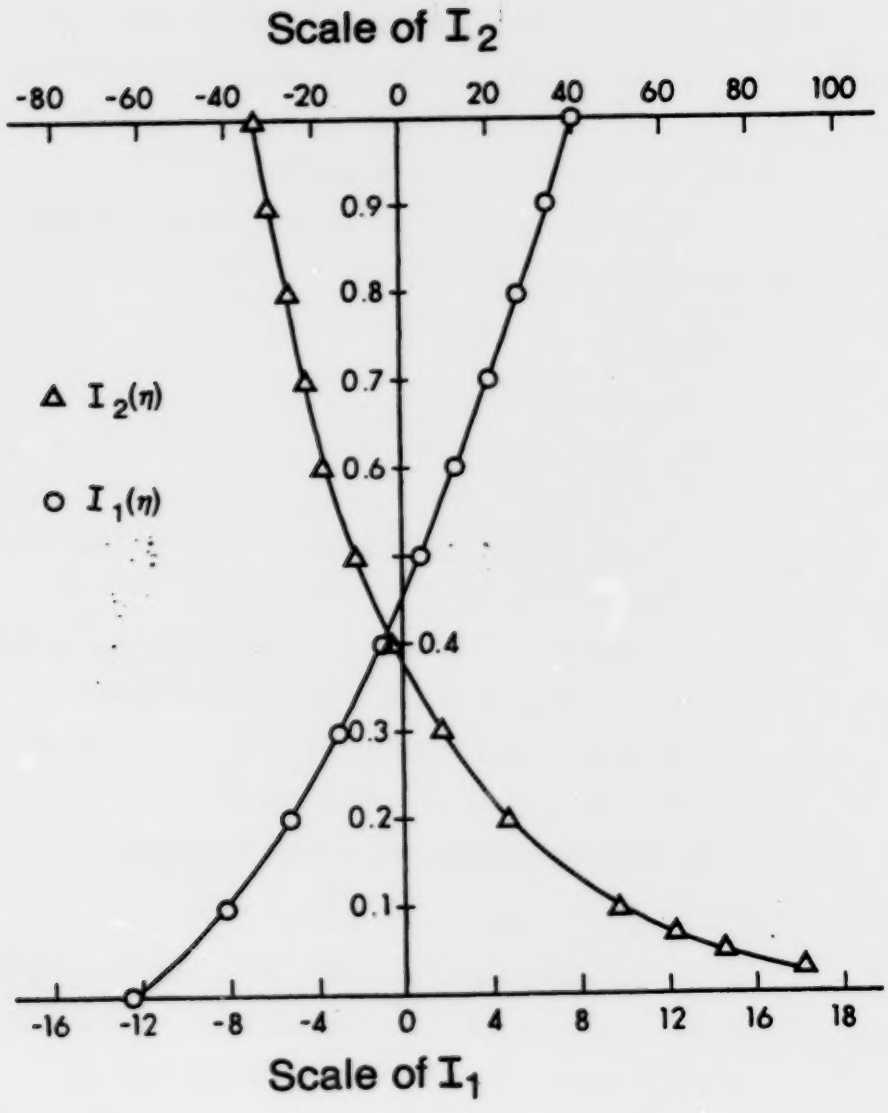

Figure 6. Integral Functions $I_1(\eta)$ and $I_2(\eta)$

The corresponding development length for superelevation was noted in Equation 33. Thus the ratio is:

$$\frac{L_B}{L_S} = \frac{1}{2C_+} \frac{B}{H_0} \tag{59}$$

For channels with aspect ratios (B/H_0) of 20 to 40, the two lengths are of similar size. For larger aspect ratios (and rougher channels) the secondary flow development is faster and the overall development is governed by the superelevation development. For smaller aspect ratios or smoother channels (typical of laboratory situations) the secondary flow development governs.

At the bend exit the same situation applies in reverse and the decay lengths are the same as above.

2.4 LONGITUDINAL VELOCITY REDISTRIBUTION

The longitudinal component of velocity is significantly affected by the curvature of the stream. As the flow enters the bend, the velocity on the inside increases while the velocity on the outside decreases. As the flow proceeds around the bend, the lateral profile becomes uniform again and then begins skewing to the outside. If the bend is long enough, equilibrium may be reached. Near the exit of the bend, a major redistribution toward the outer wall takes place. This exit redistribution is equal but opposite to the entrance redistribution. Thus the largest "skewness" of the lateral velocity profile is actually observed just past the end of the bend. Figure 7 from Rosovskii (1961) illustrates this process graphically.

There are several different mechanisms causing this phenomenon and each will be discussed separately. In the following, the longitudinal velocity referred to is taken to be the depth averaged velocity, U, defined previously.

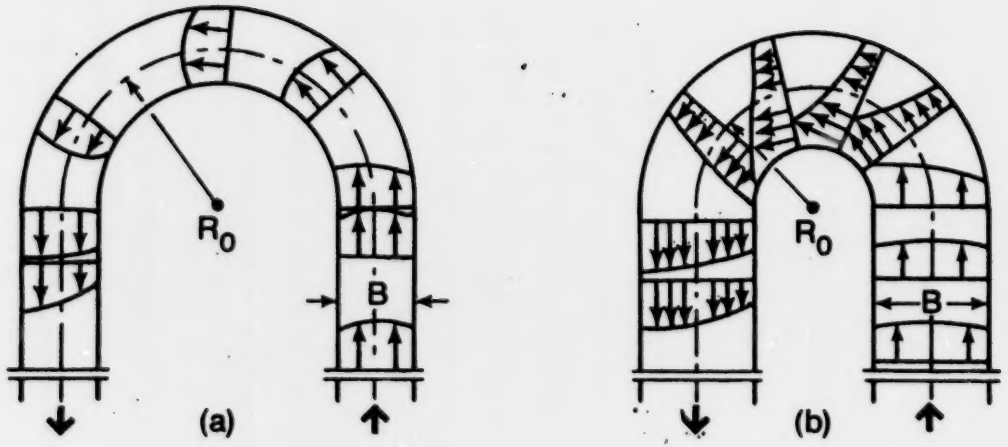

Planview of Channel Flow: (a) Weakly Curved: (b) Strongly Curved [after Rozovskii]

Figure 7. Redistribution of Longitudinal Velocity

2.4.1 Inertial Effects

Over a short distance near a change in curvature, a velocity redistribution takes place that is essentially independant of friction. This results in the free vortex velocity distribution and may be considered simply a conservation of vorticity from the first curvature to the second.

To calculate this effect, consider the specific energy along a streamline:

$$E = h_1 + \frac{U_1^2}{2g} = h_2 + \frac{U_2^2}{2g} \tag{60}$$

Point 1 is in the straight reach upstream of the bend and point 2 is in the bend. Differentiate 60 with respect to r:

$$\frac{d}{dr}\left(h_1 + \frac{U_1^2}{2g}\right) = 0 = \frac{d}{dr}\left(h_2 + \frac{U_2^2}{2g}\right) \tag{61}$$

But we know already from equation 8 that:

$$\frac{dh_2}{dr} = -\frac{U_2^2}{r} \tag{62}$$

Thus:

$$\frac{dU_2}{dr} = -\frac{U_2}{r} \tag{63}$$

integrating:

$$U_2 = \frac{U_0 R_0}{r} \tag{64}$$

as expected.

At a bend exit, we may apply the same analysis. Point 3 is before the end and point 4 is after the end:

$$\frac{d}{dr}\left(h_3 + \frac{U_3^2}{2g}\right) = \frac{d}{dr}\left(h_4 + \frac{U_4^2}{2g}\right) \tag{65}$$

For simplicity U_3 is assumed to be uniformly distributed. Thus:

$$\frac{dh_3}{dr} = \frac{d}{dr}\left(\frac{U_4^2}{2g}\right) \tag{66}$$

Again:

$$\frac{dh_3}{dr} = \frac{U_0^2}{gr} = \frac{U_4^2}{gr} \tag{67}$$

then:

$$\frac{dU_4}{dr} = \frac{U_4}{r} \tag{68}$$

and finally:

$$U_4 = \frac{U_0 r}{R_0} \tag{69}$$

From the point of view of vorticity the phenomenon may be explained as follows. Initially the flow is uniform across the channel (neglecting the sidewall regions). Its vertical vorticity is therefore zero. After entering the bend, the flow is constrained to move basically concentrically. This may be achieved without altering the vorticity only if the lateral profile assumes the form of an irrotational (free) vortex.

Friction, of course, acts to change the vorticity but it requires a significant length to cause an appreciable change. In this case it would act to make the profile more uniform. Since the flow is moving concentrically, a uniform distribution implies that the flow contains vorticity. This is evident after the end of the bend where the velocity profile skews outward.

As is obvious from the above, the inertial velocity redistribution is closely associated with the superelevation. We expect, and in fact notice, that the development lengths for velocity redistribution and superelevation are about the same. This applies to both the entrance and exit of the bend.

2.4.2 Slope Differential Effect

Referring to Figure 8, we observe that for a given arc θ flow on the outside must travel further than on the inside. Presumably, however, the change in the bed elevation will be the same from A to B. Or:

$$S_0 = \frac{\Delta z_b}{\Delta x} = \frac{\Delta z_b}{r\theta} \tag{70}$$

For the channel centreline:

$$S_{0c} = \frac{\Delta z_b}{R_0 \theta} \tag{71}$$

Therefore:

$$S_0 r = S_{0c} R_0 \tag{72}$$

Thus the slope is steeper on the inside of the channel. To estimate the effect on the lateral distribution of longitudinal velocity, consider the uniform flow approximation:

$$U = C_+ u = C_+ \sqrt{gdS_0} \tag{73}$$

Substituting Equation 72:

$$U = C_+ \frac{\sqrt{gdS_{oc} R_0}}{\sqrt{r}} \tag{74}$$

But

$$U_C = C_+ \sqrt{gdS_{0c}} \tag{75}$$

Thus:

$$\frac{U}{U_C} = \sqrt{\frac{R_0}{r}} \tag{76}$$

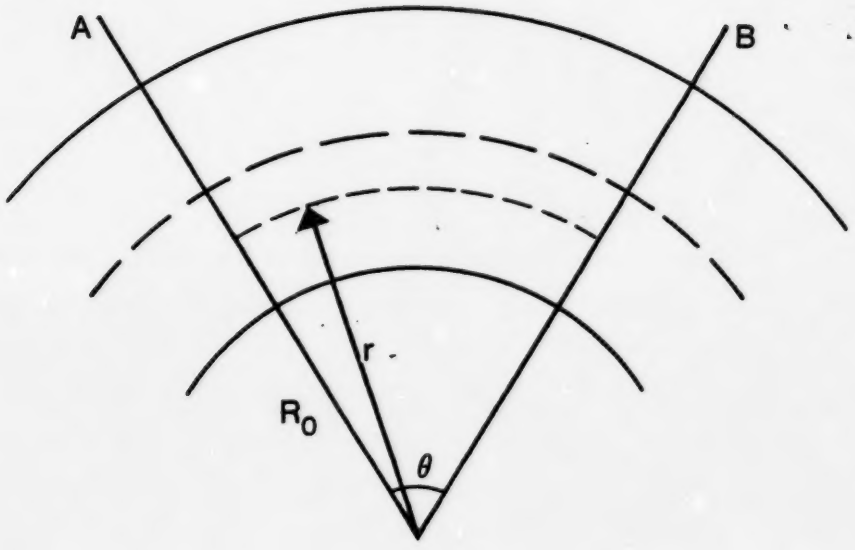

Figure 8. Slope Differential

assuming d is constant.

Equation 76 indicates that, if the slope differential were the only important factor, then, after some distance, the flow would still be faster on the inside but the variation across the channel would be reduced. This implies that the flow gains vorticity.

2.4.3 Depth of Flow (Vertical Friction)

In a similar manner to the above, we may include the effect of a non-uniform bed profile. In Equation 74 let d be a function of r to obtain:

$$\frac{U}{U_C} = \sqrt{\frac{\overline{R_0}}{r}}\ \sqrt{\frac{\overline{d}}{d_C}} \tag{77}$$

Thus the flow is faster where the water is deeper. In natural bends, it is almost invariably observed that the outside of the bend is scoured deeper than the normal depth while deposition occurs on the inside of the bend. Therefore, in natural channels a strong skewing of velocity toward the outside wall may take place.

2.4.4 Lateral Friction

The ultimate effect of lateral friction would be to cause the flow to move as a rigid body around the bend. This would require that the lateral profile be given by the forced vortex equation:

$$\frac{U}{U_C} = \frac{r}{R_C} \tag{78}$$

This effect, however, is not very strong as may be shown by consideration of the magnitude of the lateral stress gradient compared to the vertical stress gradient. The vertical stress gradient may be estimated by:

$$\varepsilon \frac{\partial^2 u}{\partial z^2} \sim \varepsilon \frac{U_0}{H_0^2} \tag{79}$$

while the lateral gradient is:

$$\varepsilon \frac{\partial^2 u}{\partial y^2} \sim \varepsilon \frac{U_0}{B^2} \qquad (80)$$

Thus the lateral stress gradient over the vertical stress gradient is proportional to $(d/B)^2$ and, since aspect ratios of natural channels are of the order 10 to far greater, the lateral friction cannot have much effect.

Near the banks, lateral friction becomes much more important, especially in slowing down the initial fast flow on the inside bank. Otherwise it has little but local effect, although it is useful to note that it does act in such a way as to shift the location of maximum velocity away from the inside of the bend.

2.4.5 Lateral Momentum Transport by Secondary Flow

The secondary circulation effect on the longitudinal flow is the least understood, but in some cases the most important, mechanism of flow redistribution. Essentially the secondary flow convects faster moving upper layer flow toward the outside while moving the slower bed layer flows toward the inside. Of itself, this accomplishes nothing since the fluid is merely replacing other fluid of similar momentum. If there is a velocity gradient across the channel, then the lower transport will act to partially counteract the upper transport.

When the fluid nears the walls, however, the vertical transport becomes important and the effects are significant. At the outer wall, fast fluid (continuously replenished from the centre of the channel) is convected downward causing an increase in mean velocity, while the opposite occurs on the inside. The effect, first noticed near the walls, would be convected again by the secondary flow towards the centre. Kalkwijk and de Vriend (1980) took this effect partially into account while only the more or less complex numerical analyses of Rosovskii (1961), Leschziner and Rodi (1979), and de Vriend (1981) take full account.

At present, the only results are qualitative and suggest that this effect is more important for channels of small aspect ratio (narrow channels) and also more important for smooth channels simply because frictional effects are smaller

by comparison. Therefore, this effect would be much more important in a laboratory flume than in a natural stream.

2.4.6 Developing Flow

As may be observed from the above, there remains much that is unquantified regarding the problem of longitudinal velocity redistribution. This makes the situation of developing flow very difficult to handle in a practical manner. It has been observed that the majority of every bend, even in the laboratory, is in a developing situation with regard to the longitudinal velocity distribution. The superelevation and secondary flow develop quickly and remain fairly stable but the longitudinal flow develops slowly. Further, it is the rare natural bend that maintains a constant curvature. For these reasons, a model of developing flow is desired. Short of using a three-dimensional numerical model, a reasonable approximation is (Engelund 1974):

$$\frac{\partial U'}{\partial x} = - y \frac{d}{dx} \left(\frac{1}{R_0}\right) - \frac{1}{C_+^2 H_0} (2U' - H') \qquad (81)$$

where:

$$U' = \frac{U-U_0}{U_0} \qquad (82)$$

$$H' = \frac{d-H_0}{H_0} \qquad (83)$$

This model takes account of some inertial and bed friction effects for channels with a lateral bed slope. It is, therefore, a good approximation for wide natural streams.

2.5 BED SHEAR STRESS

Another important area of concern is the bed shear stress distribution. Ippen and Drinker (1962) and various others have studied this problem, experimentally at least.

As a first approximation, we may take:

$$\frac{\tau_{x0}}{\rho} = u_+^2 = \frac{U^2}{C_+^2} \tag{84}$$

and assume C_+ to be a constant or a function of the relative roughness (k_s /d).

From Equation 84 and what we know from the previous section about the behaviour of U, we can qualitatively predict the bed shear stress distribution. The shear stress would be maximum near the inside wall at the beginning of the bend, then shift to the outside wall, and finally reach a peak near the outside wall just past the end of the bend. This is in fact what we observe in Figure 9 for example (Ippen and Drinker 1962).

The correlation is reasonable, but consistent discrepancies do occur. For example, the stress near the inside wall is usually somewhat lower than predicted while the stress near the outside wall is somewhat larger. Clearly, this is an effect of the secondary flow on the velocity distributions themselves. Only in the complex numerical models has this been accounted for.

The lateral bed stress arising from the secondary flow itself was evaluated previously as:

$$\tau_{y0} = \tau_{x0} \, K \, \frac{d}{r} \tag{85}$$

The total shear stress (magnitude) is therefore:

$$\tau_0 = \sqrt{\tau_{y0}^2 + \tau_{x0}^2} = \tau_{xo} \sqrt{1 + (K\frac{d}{r})^2} \tag{86}$$

Even if we take K to be 11, as suggested previously, for any natural stream

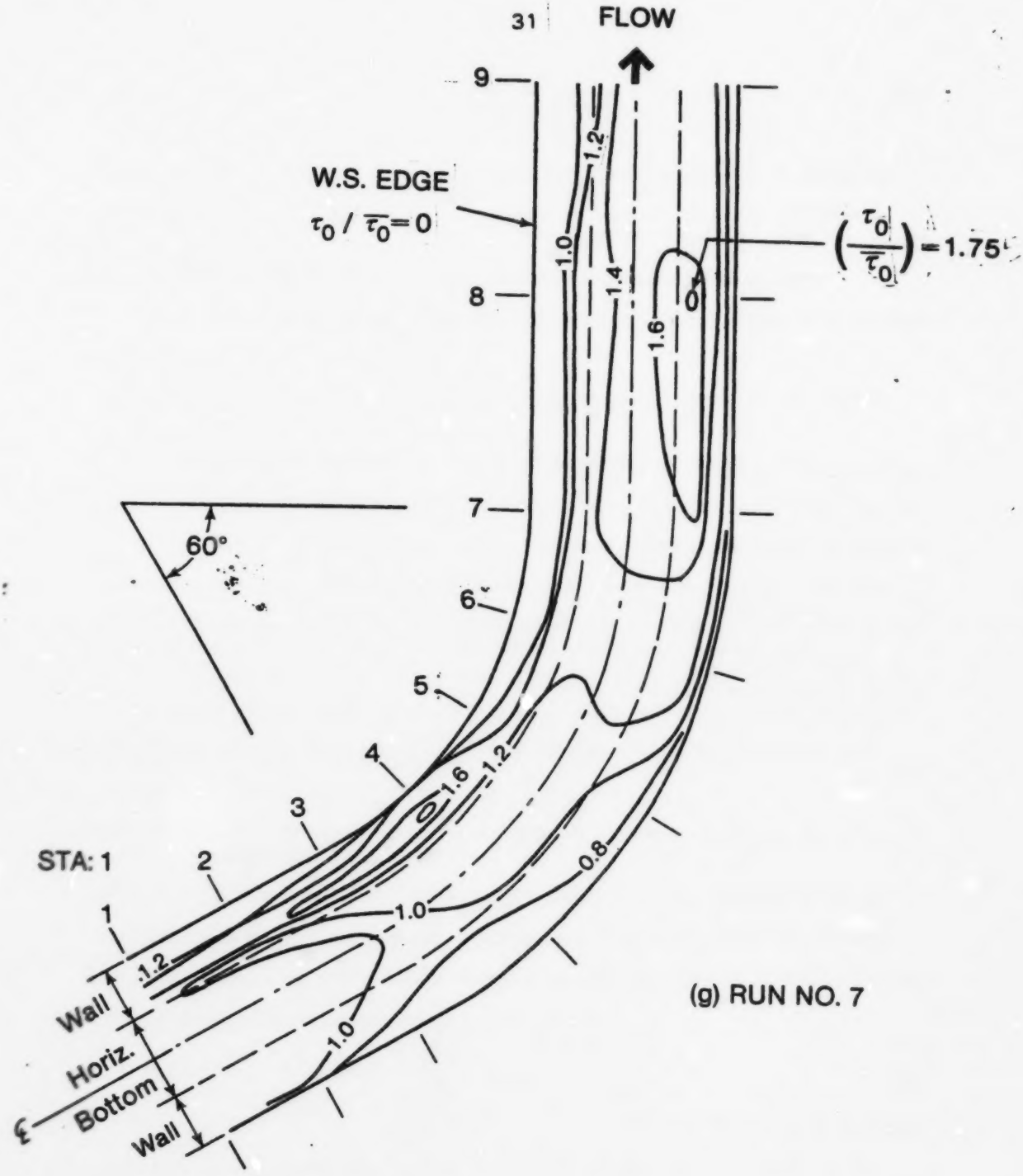

Figure 9. Bed Shear Stress Distribution (from Ippen & Drinker 1962).

$$\tau_0 = \tau_{x0} \tag{87}$$

2.6 WALL SHEAR STRESS

Wall shear stresses are even less well understood, despite their importance in bank protection works. The only approach available seems to be:

$$\frac{\tau_w}{\rho} \propto U_w^2 \tag{88}$$

where U_w is the velocity extrapolated (by eye) to the wall (as if there were no boundary layer). For cases of natural or non-rectangular channels even this approach becomes doubtful.

2.7 FRICTION COEFFICENT

The average shear stress across the bed is related to the overall friction coefficient as follows:

$$\frac{\overline{\tau_0}}{\rho} = \frac{1}{C_{+0}^2} U_0^2 \tag{89}$$

If we average Equation 84 across the channel we obtain (assuming C_+ is constant):

$$\frac{\overline{\tau_0}}{\rho} = \frac{1}{C_+^2} (\overline{U^2}) \tag{90}$$

Let:

$$U = U_0 + U_0 U' \tag{91}$$

Substitute Equation 91 into 90:

$$\frac{\overline{\tau_0}}{\rho} = \frac{U_0^2}{C_+^2} (1 + \overline{U'^2}) \tag{92}$$

Simplify to obtain:

$$\frac{C_{+0}^2}{C_+^2} = \frac{1}{(1 + \overline{U'^2})} \tag{93}$$

indicating that the overall friction coefficient will decrease (apparently increasing roughness), depending upon the skewness of the velocity. Equation 93 may be approximated by:

$$C_{+0}^2 = C_+^2 \ (1 - \overline{U'^2}) \tag{94}$$

which may be used to evaluate the overall friction coefficient if the distribution of U is known.

2.8 BED SCOUR AND TOPOGRAPHY

Since we now have at least a reasonable idea of the flow field in a bend, the next step is to attempt to predict the stable bed topography or scour pattern. Since, of course, the bed topography affects the flow field which in turn affects the bed topography, we expect that a succesive approximation technique will be required. The method outlined below, which follows Engelund (1974), will be to first estimate the bed profile at a developed section, and then estimate developing effects to apply a correction.

2.8.1 Developed Bed Profile

Under developed conditions, the net rate of sediment transport across the channel is zero. Thus the forces acting on a sediment particle must balance. Figure 10 shows the lateral forces acting on a sediment particle on the bed of a curved stream. The simplest force balance will be:

$$(W - F_L) \sin \alpha = F_{DR} \tag{95}$$

where W is particle weight, F_L is lift force, α is lateral bed angle and F_{DR} is lateral drag force. F_{DR} is assumed to be proportional to bed shear stress:

$$F_{DR} = F_{DL} \tan\delta \tag{96}$$

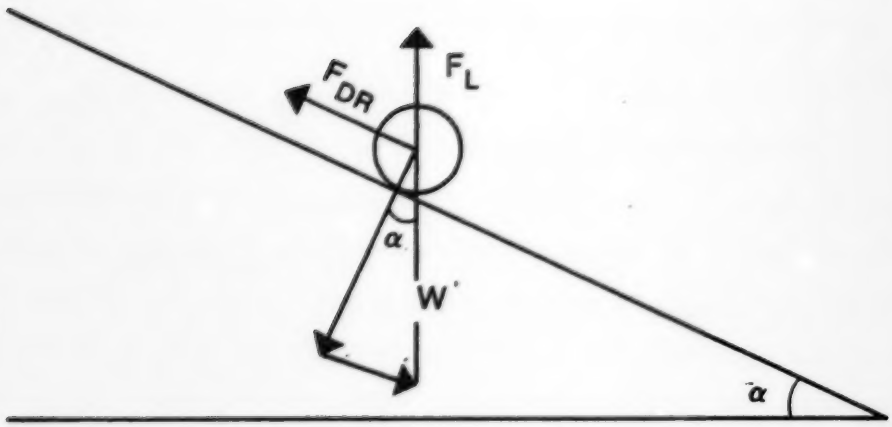

Figure 10. Particle Equilibrium

where F_{DL} is longitudinal drag force. F_{DL} may be estimated, if the particle is moving longitudinally at a constant speed, as:

$$F_{DL} = (W - F_L) \cos\alpha \tan\Phi \tag{97}$$

where Φ is the dynamic friction angle (about 25°). Substitute 97 into 96 to obtain:

$$(W - F_L) \sin\alpha = (W - F_L) \cos\alpha \tan\Phi \tan\delta \tag{98}$$

or:

$$\tan\alpha = \tan\Phi \tan\delta \tag{99}$$

Since:

$$\tan\alpha = \frac{dd}{dr} \tag{100}$$

Equation 99 becomes:

$$\frac{dd}{dr} = K \tan\Phi \frac{d}{r} \tag{101}$$

Solve the differential equation:

$$d = C\, r^{(K\tan\Phi)} \tag{102}$$

Substitute y for r and solve for C to obtain:

$$\frac{d}{H_0} = \left(1 + \frac{y}{R_0}\right)^{K \tan\Phi} \tag{103}$$

The maximum depth of scour is:

$$\frac{d_m}{H_0} = \left(1 + \frac{B}{2R_c}\right)^{K \tan\Phi} \tag{104}$$

For moderate curvature ratios ($B/R_c < 0.5$) Equation 104 may be approximated as:

$$\frac{d_m}{H_0} = 1 + \frac{K}{2} \tan\phi \frac{B}{R_0} \qquad (105)$$

Taking K as 11 and Φ as 25°, the above becomes:

$$\frac{d_m}{H_0} = 1 + 2.5 \frac{B}{R_0} \qquad (106)$$

This was derived assuming vertical sides and has been found to be very conservative. An average of field observations (Suga 1963, cited by Ikeda et al. 1981) gives a constant of approximately 1.5. Figure 11 shows a plot of Equations 104 and 106 with the modified constant against observed values for the North Saskatchewan River (data from Nwachukwu and Neill 1972). The average depth and width were evaluated at a stage corresponding to a discharge of 100 000 cfs.

Other attempts at predicting stable developed bend scour have been made by Kikkawa et al. (1976) ,Koch (1980), and Yen (1970). These involve more complete evaluations of the force balances but result in the necessity of numerical integration and require more detailed information about the flow field.

To obtain the bed topography for the entire bend, including developing effects, the only approach taken so far is due to Engelund (1974). The procedure is to set the first estimate of bed topography equal to a series of developed profiles depending on local curvature. The longitudinal velocity field is then calculated using equation 81. The mean lateral velocities are calculated from a continuity equation. Finally, a sediment conservation equation is solved numerically and the correction is applied to the initial estimate. Engelund originally derived this method for use on a channel with a sinusoidally varying radius of curvature and obtained reasonable results compared with the experiments of Hooke (1974). The method may be generalized to other meander patterns.

Generally, the results for sinusoidal channels indicate the following:

1. The deepest scour is usually somewhat downstream of the point of maximum curvature.

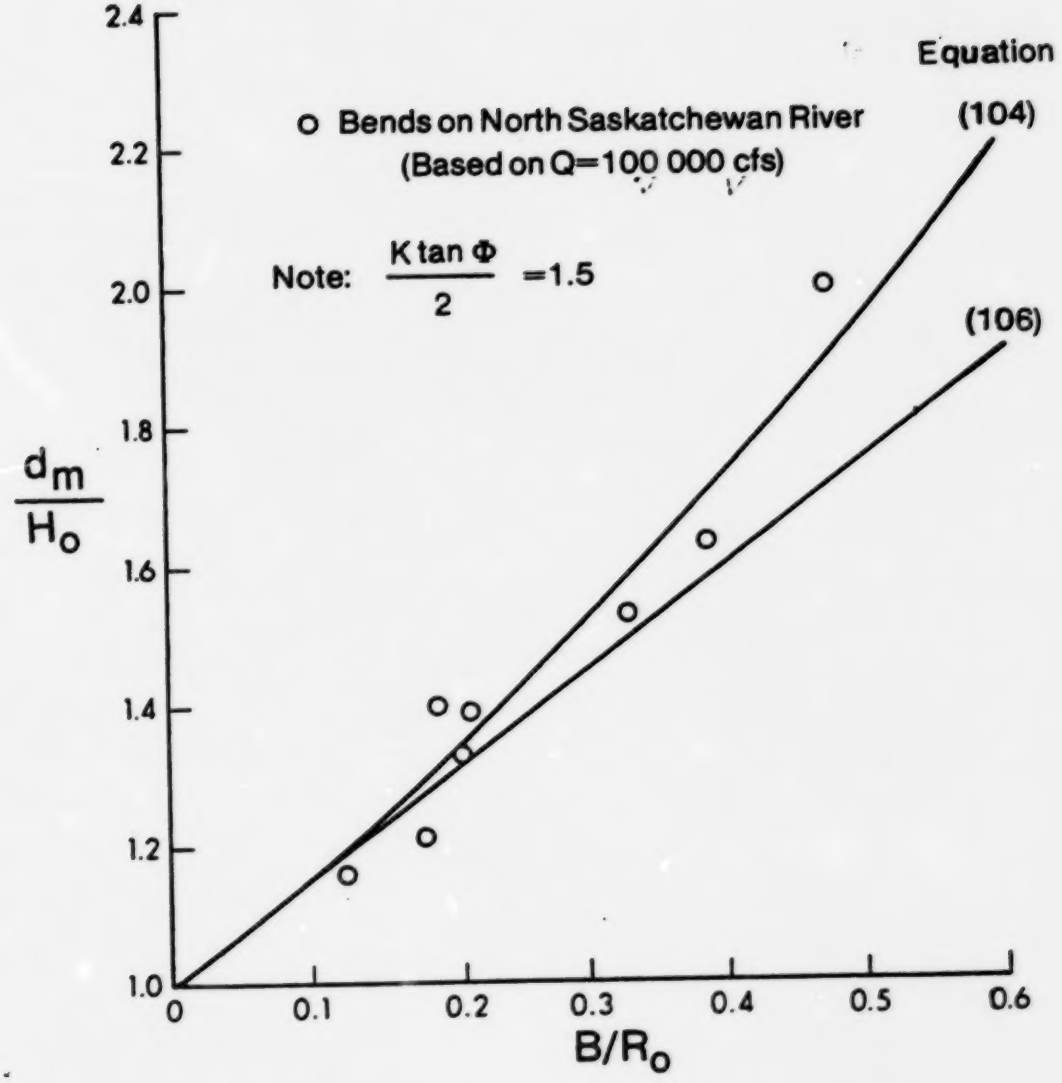

Figure 11. Maximum Scour vs. Curvature Ratio

2. The tip of the point bar (deposition) is usually even further downstream.

Both the theoretical and experimental work supports these conclusions. A more detailed evaluation of this method is included in a section 4.3.

3. REVIEW OF EXPERIMENTAL INVESTIGATIONS

Many researchers have undertaken studies on various aspects of curved open channel flow. Due to the complexity of the problem, and its many manifestations, the experimental purposes and designs are as diverse as the number of experimenters. Broadly, the experiments may be classified into three categories:

1. Fixed boundary channels;
2. Mobile boundary channels; and
3. Natural streams.

Yen (1965) gives a review of experimental work prior to his own. Included in this report is an update to that review containing the important experiments published up to 1980. Table 1 summarizes rigid boundary experiments. Table 2 is concerned with mobile bed results and Table 3 presents field observations of natural streams. An overall evaluation of the experiments is also included.

3.1 FIXED BOUNDARY CHANNELS

Most fixed boundary channels were constructed for one of two reasons. First, as general experiments to understand curved channel flows, and second to evaluate the bed stress distribution for a particular situation. Thus some experiments include detailed information on many aspects of the flow while others are very limited. Therefore the diversity in the important geometrical and flow parameters is not as large as it appears. Additionally, some of the experiments have unrealistic values of some parameters. A low aspect ratio ($B/H_c < 5$) is the most obvious example, although a low ratio R_o/H_o is unrealistic as well.

Secondary velocities have not often been measured due to their relatively small size. When measured, the lateral velocities have universally been determined by measuring the total horizontal velocity and the angle of deviation from the longitudinal direction. Usually the angle is measured by lining up a protractor-like device with a short thread in the flow.

Table 1. Rigid boundary curved channel experiments.

Investigator	Channel Plan	Cross Section	#exps	R_o/B	B/H_o	R_o/H_o	F	$R(\times 10^{-4})$	Notes
Raju[a]	1 90°bend	rectangular	nd	1. to 3.	1.6 to 4.3	nd	<1	1.5 to 4.5	loss coefficent
Boss[a]	1 90° bend	rectangular	2	2.16	3.33, 2.72	6.1, 5.9	0.64, 0.48	3.6, 3.4	superelevation
Yarnell and Woodward[a]	1 180° bend	rectangular	nd	1.0 to 2.5	0.67 to 1.33	1.07 to 1.67	0.6 to 0.7	4.2 to 6.8	u vel, superelevation
Mockmore[a]	2 180° bends	rectangular	2	1.17	3.2, 4.0	3.75, 4.6	0.15, 0.14	1.7, 1.3	u vel, superelevation
Shukry[a]	1 bend of variable angle	rectangular	nd	0.5 to 3.0	0.83 to 1.67	0.42 to 5.0	0.1 to 0.8	0.10 to 0.78	u,v vel, superelevation
Prus-Chacinski[a]	5 45° bends	rectangular	1	6.5	4.4	6.5	nd	0.55	spiral motion
Einstein and Harder[a]	1 120° bend	rectangular	nd	7.5	4.9 to 12.2	37. to 91.	0.2 to 0.4	0.5 to 1.3	u vel distribution
Leopold, Bagnold, Wolman and Brush[a]	sinusoidal	trapezoidal 1:1 side slopes	nd	nd	2.9 to 4.3	nd	0.2 to 0.9	1.4 to 2.4	resistance
Ippen, Drinker, Jobin, and Shemdin[a]	1 60° bend	trapezoidal 2:1 side slopes	nd	2.5, 5.8	3.0 to 8.0	9.9 to 34.7	0.32 to 0.55	1.1 to 7.5	u vel, superelevation, boundary shear

continued...

Table 1. Continued.

Investigator	Channel Plan	Cross Section	#exps	R_o/B	B/H_o	R_o/H_o	F	R(x 10^{-4})	Notes
Milovich[a]	1 180° bend	rectangular	nd	1.16	1.7 to 5.3	2.0 to 6.2	<1.0	0.016 to 0.12	bottom velocity, surface velocity
Danelia[a]	1 180° bend	rectangular	1	1.5	3.33	5.0	0.28	2.1	u, v vel. distributions
Kozhevnikov[a]	1 to 3 180° bends	rectangular, trapezoidal, triangular	nd	2.0	6.7 to 40.0	13.3 to 90.0	0.2 to 0.7	0.23 to 1.5	bottom velocity, surface velocity, superelevation
Ter-Asvatsatryan[a]	1 bend 67.5°, 180°	rectangular	nd	1.5 to 5.5	2.5 to 3.5	3.85 to 19.0	0.3 to 0.4	1.8 to 3.2	u, v vel. distributions
Konovalov, Makkaveev, and Romanenko[a]	sinusoidal	trapezoidal	nd	nd	3.8 to 8.3	nd	0.2 to 0.3	0.7 to 1.4	bottom and surface velocities
Makkaveev and Romanenko[a]	sinusoidal	rectangular	nd	>2.0	2.0 to 10.0	>4.17	<1.0	0.4 to 4.0	bottom and surface velocities
Fidman[a]	3 117.5° bends	rectangular	nd	2.25	6.25 to 8.33	14.0 to 19.5	0.07 to 0.3	0.9 to 3.8	superelevation
Ananyan[a]	2 180° bends	rectangular	nd	5.0	4.8 to 5.3	2.8 to 3.3	0.21 to 0.28	2.4 to 3.1	u, v vel. distribution
Rozovskii[a]	1 bend 29° to 180°	rectangular, triangular	nd	1.0 to 2.5	4.3 to 27	5.3 to 45.0	0.2 to 0.5	0.028 to 2.7	u, v vel, superelevation

continued...

Table 1. Continued.

Investigator	Channel Plan	Cross Section	#exps	R_o/B	B/H_o	R_o/H_o	F	$R(\times 10^{-4})$	Notes
Siebert and Gotz (1975)	3 180° bends	rectangular	2	4.6, 20.	18.2, 80.	0.23	2.5, 20.		long. dist. of u and v vel.
Yen and Yen (1971)	2 90° bends	trapezoidal	1	4.7	nd	nd	nd	nd	water surface configuration
Fox and Ball (1968)	1 180° bend	rectangular	1	3.5	2.0	7.0	0.25	5	u , v distributions
Kikkawa, Ikeda, Kitagawa (1976)	1 330° bend	rectangular	3	4.5	15.9 to 20	71.4 to 90	0.56 to 0.63	2 to 3	u,v at 180° meas. bed stress at 6 sections
Yen (1965)	2 90° bends	trapezoidal 1:1 side slopes	5	4.67	8.0 to 17.0	41.5 to 83.8	0.36 to 0.82	6.3 to 13.8	u, v velocites, superelevation, bed stress
Varshney and Garde (1975)	1 60° bend	rectangiular	84	1.5 to 6.0	2.06 to 11.95	3.09 to 83.70	0.11 to 0.78	2.27 to 10.9	various roughness, bed stress only
Choudhary and Narasimhan (1977)	1 180° bend	rectangular	6	0.833	5, 10	4.2 to 8.3	0.2 to 0.6	4.10	u,v,h and bed stress
Soliman and Tinney (1968)	1 180° bend	rectangular	6	0.625	1.2 to 1.5	0.75 to 0.94	0.35 to 0.58	nd	h, used guide vanes

continued...

Table 1. Concluded.

Investigator	Channel Plan	Cross Section	#exps	R_o/B	B/H_o	R_o/H_o	F	R(x 10^{-4})	Notes
Zimmerman (1977)	1 330° bend	rectanguular	6	5.5	2.10 to 36.7	3.8 to 6.7	0.22 to 0.35	6.7 to 16.0	measured only at 0.2 cm above bed for various roughness
Zimmerman (1977)	1 330° bend	rectangular	6	4.25	27.5 to 55.0	5.0 to 10.0	0.21 to 0.39	3.6 to 9.2	same as above but 1 roughness only
Kalkwijk and deVriend (1980) & (1978)	1 90° bend	"natural"	2	8.3	250.0	30.0	0.14 to 0.28	nd	depth averaged velocities & water surface elevations

[a] Adapted from original table in Yen (1965)

Table 2. Mobile boundary curved channel experiments.

Investigator	Channel Plan	#exps	R_c/B	R_c/H_c	B/H_c	F	R(x 10^{-4})	D_{50}(mm)	Notes
Zimmerman (1977)	1 330° bend	12	3.0 to 5.5	21.1 to 40.4	5.6 to 8.85	0.23 to 0.48	4.1 to 9.6	0.21	angle of ripples to obtain bed stress angle
Hooke (1974)	sinusoidal	5	2.46 (using min radius)	20.2 to 48.4	8.2 to 19.6	0.27 to 0.40	nd	0.30	bed topography, shear stress, sediment discharge
Yen (1970)	2 90° bends	5	4.7	nd	18.0 to 30.0	0.30 to 0.70	7.0 to 14.0	0.25	topography, velocities, shear stress
Zimmerman and Kennedy (1978)	1 330° bend	49	3.0 to 5.5	16.7 to 55.6	5.4 to 10.0	nd	nd	0.21, 0.55	transverse bed slopes and sediment discharge
Onishi, Jain and Kennedy (1976)	2 90° bends	26	3.6 to 7.3	62.5 to 110.3	8.63 to 30.2	0.28 to 0.56	10.3 to 26.6	0.25	friction factor and sediment discharge
Kikkawa, Ikeda, Kitagawa (1976)	1 330° bend	2	4.5	71.4 to 81.8	15.9 to 18.2	0.61 to 0.63	nd	0.90	bed profiles (time variation)

Table 3. Natural stream bend measurements.

Investigator	River	Q (m^3/s)	Notes
Bridge and Jarvis (1977)	South Esk (Scotland)	3.0 to 22.0	measured velocity profiles and bed stresses in a gently curving stream.
Bathurst, Thorne, and Hey (1979)	Severn (Wales)	1.0 to 15.5	measured velocity (longitudinal and transverse) and shear stress at four locations.

The error in these measurements is relatively large. Vertical velocity measurements are practically nonexistent.

The only turbulence measurements reported are those of Yen (1965), but these were taken in a closed air duct model. Some measurements, especially of the turbulent Reynold's stresses, would be very useful.

An interesting result of these experiments is that only in the configuration of Kikkawa et al. was a convincing demonstration of a fully developed situation achieved. The total angle turned by their flume was over 300 degrees.

3.2 MOBILE BOUNDARY CHANNELS

Most mobile boundary curved channel experiments were set up to investigate the bed topography. Typically the bed is initially flat and then the experiment run until an equilibrium bed topography is reached. The bed elevations, and in some cases various flow variables, are then measured.

Many of the same criticisms applied to the rigid boundary channels may also be applied to the mobile channel. Additionally, it should be noted that all these experiments utilized rigid vertical walls. This results in considerable distortion of the bed topography near the outside wall. Also, to measure mean bed topography, it was often necessary to smooth local bedforms, which may intoduce further distortions.

3.3 NATURAL STREAM OBSERVATIONS

Detailed studies of natural stream bends are notable by their relative scarcity. The complexity and uncontrolled nature of the situation limit the utility of the results. Measurements of this kind are very important in validation of theoretical or experimental conclusions. It is, however, difficult to obtain general results from them.

4. MATHEMATICAL MODELS

To calculate maximum scour, superelevation, and secondary flow, the developed flow assumption appears to be adequate, provided that a representative curvature can be obtained. For more detailed studies requiring bed topography and flow distribution over a reach of a natural or artificial channel, this simple approach is inadequate. A more complex physical or mathematical model is required. As curvature presents no special difficulties to a properly scaled and constructed physical model, we will focus our attention on mathematical models.

At present, no complete mathematical model is available, but some attempts have been made at solving various aspects of the problem. This section will briefly consider these approaches in order of decreasing complexity.

4.1 THREE-DIMENSIONAL MODELS

A fully three-dimensional model based on the full Reynold's equations and appropriate boundary conditions would be the most complete possible. Difficulties arise, however, in the modelling of the turbulent stresses. Rodi (1980) gives a review of the possibilities, ranging from simple constant eddy viscosity assumptions to full two parameter turbulence transport models. Based on some consideration of the developed flow analysis we conclude that the actual turbulence model chosen is not that significant. For example, the secondary circulation profile obtained by assuming a mixing length model (Rosovskii 1961) does not differ greatly from that obtained using an average eddy viscosity model (Engelund 1974). Rodi (1980) points out this observation as well when considering a developing strongly curved flow.

The three-dimensional model of Leschizner and Rodi (1979) uses the $\kappa - \epsilon$ turbulence transport model. This model, although the most complete yet attempted, contains some simplifications. First, the variable water surface location is ignored in the calculation. That is, an imaginary frictionless lid is placed over the flow. The water elevations are calculated later from the pressure distributions. The effect of this simplification is to limit the model to situations where the

Froude number is small.

A second simplification was made with regard to longitudinal derivatives of the turbulent stresses. These were neglected, leaving only the pressure as an effective downstream-to-upstream mechanism. This allows a storage efficient calculation procedure, where the pressure field is first assumed, and then the calculation is performed starting at the beginning and proceeding downstream. The scheme requires the storage of only cross-sectional velocity and turbulence values, reducing computer memory requirements considerably.

This model achieved good agreement with an experiment of Rosovskii (1961) where the relative curvature was large ($B/R_c = 1$) and the Froude number was small ($F = 0.1$). The channel shape was rectangular with rigid sides and bed. As yet, no three-dimensional model includes sediment transport features.

4.2 TWO-DIMENSIONAL MODEL

A two-dimensional curved open channel flow model could be formed by assuming a hydrostatic pressure distribution, and depth averaging the equations of motion. Assumed vertical profiles could be used to calculate integral transfer coefficients. Such a model has been proposed by Kalkwijk and de Vriend (1980). The flow is assumed to be wide and shallow. The depth is allowed to vary gradually across the channel, and the channel need not be prismatic. The effect of secondary flow convection on the main flow distribution is included in an approximate way.

The inertia of the lateral mean flow and circulation are neglected, which restricts the model to gentle transitions of curvature and bed topography. This model was used to give a good prediction of the longitudinal flow field and superelevation in a rigid boundary flume of natural bed topography.

4.3 ONE-DIMENSIONAL MODELS

If lateral distributions may be approximated by linear functions, the problem may be simplified to a one-dimensional form. An example is the model proposed by Engelund (1974) which was partially discussed previously. The restrictions on this model are at least as severe as those on either of the more complex models. Additionally, the restriction of gentle curvature ($B/R_o < 1$) is required.

In the original paper, Engelund provided a solution for the case of sinusoidal variation of channel curvature. This may be easily generalized to an arbitrary alignment by solving Equation 69 numerically. As an example of such implementation, the program CRVCNL is presented in the appendix (Section 7). As of this writing, the Engelund model is the only one that will calculate bed topography as well. The main limitation of this calculation is that it applies to vertical rigid walls requiring some judgement to evaluate the scour depths if applied to natural streams. The bed topography calculation has been included in CRVCNL as well.

4.4 SUMMARY

Mathematical modelling of curved open channels has only recently been attempted with some positive results. None of the models presented are truly of a general purpose nature, and indeed most are quite restrictive.

5. CONCLUSIONS

This report has covered three aspects of the present knowledge concerning the subject of flow in curved open channels. The following is a brief evaluation of the state of the art in each of these aspects.

5.1 MECHANICS OF FLOW IN CURVED CHANNELS

Over the past twenty years or so, much effort has been expended attempting to understand the mechanics of flow in curved open channels. The phenomena of superelevation and secondary flow are well understood for the idealized situation of developed flow in a wide channel. Developing flow and the associated redistribution of longitudinal velocity are not well understood, and no simple predictive tools are available. Bed and wall stresses are likewise poorly understood. Equilibrium bed scour is more successfully predicted, due mainly to its dependance more upon the secondary flow than on the longitudinal flow and shear stress. Even here, the success is due to the calibration of the friction coefficient Φ, since the constant K and its variation with C_* are still the subject of considerable debate.

5.2 EXPERIMENTAL STUDIES

Many experiments have been performed, but most are faulted by a lack of scope. The nature of the problem is such that there is an enormous range of geometrical and flow variations. With a few notable exceptions, the present body of experimental data provides many geometrical variations, but with only a few aspects of the flow actually measured.

As far as the measurements themselves are concerned, there is a need for accurate lateral velocity, turbulence, and vertical velocity measurements, all of which are practically nonexistent.

5.3 MATHEMATICAL MODELS

Mathematical modelling of curved channel flows is only a relatively recent development. At present there have been some promising approaches taken. Much more effort is required, however, to extend these models to practical situations where arbitrary geometries, flow conditions, and sediment transport are important.

6. REFERENCES CITED

Bathurst, J.C., C.R. Thorne, and R.D. Hey. 1979. Secondary flow and shear stress at river bends. Journal of the Hydraulics Division, ASCE 105(HY10): 1277-1295.

Bridge, J.S., and J. Jarvis. 1977. Velocity profiles and bed shear stress over various bed configurations in a river bend. Earth Surface Processes 2:281-294.

Choudhary, U.K., and S. Narasimhan. 1977. Flow in 180° open channel rigid boundary bends. Technical note, Journal of the Hydraulics Division, ASCE 103(HY6): 651-657.

Einstein, H.A., and J.A. Harder. 1954. Velocity distribution and the boundary layer at channel bends. Transactions of the American Geophisical Union 35(1): 114-120.

Engelund, F. 1974. Flow and bed topography in channel bends. Journal of the Hydraulics Division, ASCE 100(HY11): 1631-1648.

Fox, J.A., and D.J. Ball. 1968. The analysis of secondary flow in open channels. Proceedings, Institution of Civil Engineers 39:467-475.

Hooke, R.L. 1974. Shear stress and sediment distribution in a meander bend. Department of Physical Geography, University of Uppsala, Sweden, Report No. 30, 58 pp.

Ikeda, S., G. Parker, and K. Sawai. 1981. Bend theory of river meanders, part 1, linear development. Journal of Fluid Mechanics 112: 363-377.

Ippen, A.T., and P.A. Drinker. 1962. Boundary shear stresses in curved trapezoidal channels. Journal of the Hydraulics Division, ASCE 88(HY5): 143-179.

Kalkwijk, J.P.Th., and H.J. de Vriend. 1980. Computation of the flow in shallow river bends. Journal of Hydraulic Research, IAHR 18(4): 327-341.

Kellerhals, R., C.R. Neill, and D.I. Bray. 1972. Hydraulic and geomorphic characteristics of rivers in Alberta. River Engineering and Surface Hydrology Report 72-1. Edmonton: Research Council of Alberta. 54 pp.

Kikkawa, H., S. Ikeda, and A. Kitagawa. 1976. Flow and bed topography in curved open channels. Journal of the Hydraulics Division, ASCE 102(HY9): 1327-1342.

Koch, F.G. 1980. Bed level computations for axisymmetric curved channels. Delft Hydraulics Laboratory, TOW Report R657-IX/W308-1. 69 pp.

Leschizner, M.A., and W. Rodi. 1979. Calculation of strongly curved open channel flow. Journal of the Hydraulics Division, ASCE 105(HY10): 1297-1314.

Nouh, M.A., and R.D. Townsend. 1979. Shear stress distribution in stable channel bends. Journal of the Hydraulics Division, ASCE 105(HY10): 1233-1245.

Nwachukwu, B.A., and C.R. Neill. 1972. Analysis of channel regime, North Saskatchewan River, Edmonton to provincial boundary. Report REH/72/1. Edmonton: Research Council of Alberta. 75pp.

Onishi, Y., S.C. Jain, and J.F. Kennedy. 1976. Effects of meandering in alluvial streams. Journal of the Hydraulics Division, ASCE 102(HY7): 899-917.

Rodi, W. 1980. Turbulence models and their application in hydraulics. State-of-the-Art Paper, IAHR 104 pp.

Rosovskii, I.L. 1961. Flow of water in bends of open channels. Jerusalem: Israel Program for Scientific Translation. 233 pp. (Translated from Russian).

Siebert, W., and W. Gotz. 1975. A study on the deformation of secondary flow in models of rectangular meandering channels. Proceedings of the XVI Congress, IAHR. 1975 july 27 - aug 1; Sao Paulo; 2(B-18): 141-149.

Soliman, M.M., and E.R. Tinney. 1968. Flow around 180° bends in open rectangular channels. Journal of the Hydraulics Division, ASCE 94(HY4): 893-908.

Varshney, D.V., and R.J. Garde. 1975. Shear distribution in bends in rectangular channels. Journal of the Hydraulics Division, ASCE 101(HY8): 1053-1066.

de Vriend, H.J. 1976. A mathematical model of steady flow in curved open shallow channels. Communications on Hydraulics, Department of Civil Engineering, Delft University of Technology. Report No. 76-1. 116 pp.

Yen, B.C. 1965. Characteristics of subcritical flow in a meandering channel. Institute for Hydraulic Research, University of Iowa. 76 pp.

Yen, C.L. 1970. Bed topography effect on flow in a meander. Journal of the Hydraulics Division, ASCE 96(HY1): 57-73.

Yen, C.L., and B.C. Yen. 1971. Water surface configuration in channel bends. Journal of the Hydraulics Division, ASCE 97(HY2): 303-321.

Zimmermann, C. 1977. Roughness effects on the flow direction near curved stream beds. Journal of Hydraulic Research, IAHR 15(1): 73-85.

Zimmermann, C., and J.F. Kennedy. 1978. Transverse bed slopes in curved alluvial streams. Journal of the Hydraulics Division, ASCE 104(HY1): 33-48.

7. APPENDIX - PROGRAM CRVCNL

The computer program CRVCNL is a numerical implementation of the Engelund (1974) method of flow and bed topography calculation for a curved channel. The method has been generalized to allow an arbitrary meander geometry. The channel curvature is calculated from the centreline co-ordinates of the stream plan supplied by the user. The program outputs velocity (longitudinal) corrections and bed depths below the water surface as well as various intermediary calculated quantities.

This program is intended for the demonstration of the Engelund method only. Included are input instructions and a listing of the FORTRAN source code.

7.1 INPUT TO CRVCNL

FORTRAN input unit = 5

Card #1 (5F10.4)

1. Average depth of flow for a straight reach (consistent length unit);
2. Average width of stream (consistent length unit);
3. Friction factor of stream defined from:

$$f = \sqrt{\frac{2}{C_+^2}} \qquad (107)$$

4. Sediment friction angle (in degrees) ($\simeq$ 25 to 30 degrees, may be calibrated);
5. Sediment transport coefficient ($\simeq$ 4.0, may be calibrated).

Card #2 (2I3,F10.4)

1. Number of longitudinal sections (NSP);
2. Number of calculation points across channel (NNP);
3. Distance between sections (consistent length unit);

Card #3 to Card #(NSP+2) (2F10.4)

1. X co-ordinate of channel plan (consistent length unit);

2. Y co-ordinate of channel plan (consistent length unit).

These co-ordinates are determined by choosing equally spaced points along the channel and referring each point to an arbitrary Cartesian co-ordinate system with the positive x-direction corresponding roughly to downstream along the valley axis. All lengths output will be expressed in the same unit used in the data input.

7.2 OUTPUT

FORTRAN output unit = 6

The output of the various variables is similar. The longitudinal co-ordinate is printed on the left of the page while the cross channel variation of the variable is printed across the page. The distance between these points is the width divided by (NNP-1).

7.3 PROGRAM EXAMPLE

The program is demonstrated on a situation which is an idealization of the North Saskatchewan River near the Mayfair Golf Course in Edmonton. The river is represented as a single 180° bend with a centreline radius of 750 m. Flow conditions are based on the two year flood. All length dimensions are in metres. The input data file is listed on Figure 12, the final bed topography output is shown on Figure 13, and the program source code is listed on Figure 14.

```
  1      3.4,170.,0.0050,23.,4.,
  2       29   7 131.0000
  3      -655.,-750.,
  4      -524.,-750.,
  5      -393.,-750.,
  6      -262.,-750.,
  7      -131.,-750.,
  8      0.,-750.,
  9      130.,-739.,
 10      257.,-705.,
 11      375.,-650.,
 12      482.,-575.,
 13      575.,-482.,
 14      650.,-375.,
 15      705.,-257.,
 16      739.,-130.,
 17      750.,0.,
 18      739.,130.,
 19      705.,257.,
 20      650.,375.,
 21      575.,482.,
 22      482.,575.,
 23      375.,650.,
 24      257.,705.,
 25      130.,739.,
 26      0.,750.,
 27      -131.,750.,
 28      -262.,750.,
 29      -393.,750.,
 30      -524.,750.,
 31      -655.,750.,
End of file
```

Figure 12. Input for program example.

```
        CURVED CHANNEL  BED TOPOGRAPHY OUTPUT

    S(M)   BED TOPOGRAPHY

0.0         0.34000E+01 0.34000E+01 0.34000E+01 0.34000E+01 0.34000E+01 0.34000E+01 0.34000E+01
0.13100E+03 0.34000E+01 0.34000E+01 0.34000E+01 0.34000E+01 0.34000E+01 0.34000E+01 0.34000E+01
0.26200E+03 0.34000E+01 0.34000E+01 0.34000E+01 0.34000E+01 0.34000E+01 0.34000E+01 0.34000E+01
0.39300E+03 0.34000E+01 0.34000E+01 0.34000E+01 0.34000E+01 0.34000E+01 0.34000E+01 0.34000E+01
0.52400E+03 0.48958E+01 0.44388E+01 0.39938E+01 0.34078E+01 0.28188E+01 0.23578E+01 0.21898E+01
0.65500E+03 0.48938E+01 0.48588E+01 0.43018E+01 0.38618E+01 0.35618E+01 0.19078E+01 0.18918E+01
0.78600E+03 0.27688E+01 0.30628E+01 0.32098E+01 0.33248E+01 0.35188E+01 0.37878E+01 0.41778E+01
0.91700E+03 0.18988E+01 0.19898E+01 0.25448E+01 0.32718E+01 0.40888E+01 0.48958E+01 0.55888E+01
0.10480E+04 0.17098E+01 0.20478E+01 0.25028E+01 0.33018E+01 0.40858E+01 0.48988E+01 0.54488E+01
0.11790E+04 0.17428E+01 0.20888E+01 0.25428E+01 0.33238E+01 0.40488E+01 0.47808E+01 0.53588E+01
0.13100E+04 0.18008E+01 0.21478E+01 0.26008E+01 0.33388E+01 0.40208E+01 0.46788E+01 0.52908E+01
0.14410E+04 0.18058E+01 0.21578E+01 0.27038E+01 0.33478E+01 0.40188E+01 0.46578E+01 0.52348E+01
0.15720E+04 0.18508E+01 0.22028E+01 0.27378E+01 0.33698E+01 0.39938E+01 0.45058E+01 0.51688E+01
0.17030E+04 0.18528E+01 0.22068E+01 0.27448E+01 0.33698E+01 0.39888E+01 0.45988E+01 0.51688E+01
0.18340E+04 0.18308E+01 0.21898E+01 0.27398E+01 0.33648E+01 0.40008E+01 0.46088E+01 0.51708E+01
0.19650E+04 0.18058E+01 0.21718E+01 0.27328E+01 0.33588E+01 0.40118E+01 0.46238E+01 0.51888E+01
0.20960E+04 0.18518E+01 0.22128E+01 0.27588E+01 0.33728E+01 0.39908E+01 0.45788E+01 0.51388E+01
0.22270E+04 0.18768E+01 0.22388E+01 0.27738E+01 0.33748E+01 0.39778E+01 0.45858E+01 0.50998E+01
0.23580E+04 0.18858E+01 0.22458E+01 0.27808E+01 0.33788E+01 0.39728E+01 0.45448E+01 0.50898E+01
0.24890E+04 0.19258E+01 0.22818E+01 0.28018E+01 0.33788E+01 0.39538E+01 0.45088E+01 0.50358E+01
0.26200E+04 0.19098E+01 0.22668E+01 0.27968E+01 0.33788E+01 0.39608E+01 0.45208E+01 0.50528E+01
0.27510E+04 0.19408E+01 0.22958E+01 0.28118E+01 0.33778E+01 0.39468E+01 0.44938E+01 0.50178E+01
0.28820E+04 0.85888E+00 0.10498E+01 0.21928E+01 0.34228E+01 0.46288E+01 0.58908E+01 0.64428E+01
0.30130E+04 0.65878E-01 0.67008E+00 0.20418E+01 0.35848E+01 0.48148E+01 0.59218E+01 0.64988E+01
0.31440E+04 0.26738E+01 0.27098E+01 0.30388E+01 0.34318E+01 0.37888E+01 0.40988E+01 0.41688E+01
0.32750E+04 0.38248E+01 0.38198E+01 0.35668E+01 0.33398E+01 0.31878E+01 0.30618E+01 0.30218E+01
0.34060E+04 0.38108E+01 0.37278E+01 0.35418E+01 0.33638E+01 0.32078E+01 0.31218E+01 0.30638E+01
0.35370E+04 0.37258E+01 0.36638E+01 0.35208E+01 0.33638E+01 0.32088E+01 0.31898E+01 0.31448E+01
0.36688E+04 0.36608E+01 0.36138E+01 0.35018E+01 0.33798E+01 0.32798E+01 0.32098E+01 0.31878E+01
```

Figure 13. Output from program example.

```
      C
      C       CRVCNL
      C
      C
      C  PROGRAM TO CALCULATE BED TOPOGRAPHY OF A MEANDERING RIVER.
      C   USES METHOD OF ENGELUND(1974) GENERALIZED TO ALLOW
      C    ARBITRARY MEANDER GEOMETRY.
      C
      C
            IMPLICIT REAL*8 (A-H, O-Z)
            DIMENSION XM(100),YM(100),C(100),DC(100)
            DIMENSION DEP1(101,21),U(101,21),DU(101,21)
            DIMENSION V(101,21),DUI(101,21),DEPC(101,21),DEP2(101,21)
      C
      C     INPUT DATA
      C
            READ(5,100)D,B,F,PHI,P
        100 FORMAT(5D10.4)
            TPHI=7.*DTAN(PHI*3.14159/180.)
            READ(5,101)NSP,NRP,DS
        101 FORMAT(2I3,D10.4)
            DO10 I=1,NSP
            READ(5,102)XM(I),YM(I)
        102 FORMAT(2D10.4)
         10 CONTINUE
      C
      C     CALCULATE CURVATURES
      C
            NSP1=NSP-1
            DO 20 I=2,NSP1
            C(I)=DATAN((YM(I+1)-YM(I))/(XM(I+1)-XM(I)))
           *      -DATAN((YM(I)-YM(I-1))/(XM(I)-XM(I-1)))
            C(I)=C(I)/DS
            IF(XM(I).GE.XM(I-1).AND.XM(I).GE.XM(I+1))C(I)=C(I-1)
            IF(XM(I).LE.XM(I-1).AND.XM(I).LE.XM(I+1))C(I)=C(I-1)
         20  CONTINUE
            DC(1)=0.
            DC(NSP)=0.
            C(1)=C(2)
            C(NSP)=C(NSP1)
            DO 30 I=2,NSP1
         30 DC(I)=(C(I+1)-C(I-1))/2./DS
      C
            CALL OUTPUT(NSP,DS,1,'CURVATURE',8,C)
            CALL OUTPUT(NSP,DS,1,'DERIVATIVE OF CURVATURE',33,DC)
      C
      C     CALCULATE FIRST APPROXIMATION TO BED TOPOGRAPHY
      C
            DR=B/(NRP-1)
            RO=-B/2.
            DO31 I=1,NSP
            DO 31 J=1,NRP
         31 DEP1(I,J)=(1.+(J-1)*DR+RO)*C(I))*TPHI
      C
            CALL OUTPUT(NSP,DS,NRP,'FIRST DEPTH APPROXIMATION',25,DEP1)
      C     CALCULATE LONGITUDINAL VELOCITY CORRECTION
      C
            DO 32 J=1,NRP
            R=(J-1)*DR+RO
            U(1,J)=B*TPHI*C(1)/2.
            DU(1,J)=0
            DO32 I=2,NSP
            UK1=DS*(R*(-DC(I-1)*TPHI)*F/D/2.*C(I-1))-F/D*U(I-1,J))
            DU(I-1,J)=UK1/DS
            UK2=DS*(R*((-DC(I-1)-DC(I))/2.*TPHI)*F/D/4.*(C(I-1)*C(I)))-F/D
           **(U(I-1,J)+UK1/2.))
            UK3=DS*(R*((-DC(I-1)-DC(I))/2.*TPHI)*F/D/4.*(C(I-1)*C(I)))-F/D
           **(U(I-1,J)+UK2/2.))
            UK4=DS*(R*(-DC(I)*TPHI)*F/D/2.*C(I))-F/D*(U(I-1,J)+UK3))
            U(I,J)=U(I-1,J)+(UK1+2.*UK2+2.*UK3+UK4)/6.
         32 CONTINUE
      C
            CALL OUTPUT(NSP,DS,NRP,'LONGITUDINAL VELOCITY CORRECTION',32,U)
      C
      C     CALCULATE LATERAL VELOCITY
      C
            DO33 I=1,NSP
            TE=(-1.*TPHI)*DC(I)*TPHI)*F/2./D*C(I)-F/B/D*U(I,NRP)
            TI=-DC(I)*TPHI*F/2./D*C(I)-F/B/D*U(I,NRP)
            DO 33 J=1,NRP
            R=(J-1)*DR+RO
            V(I,J)=TE/2./DEP1(I,J)/(1.+C(I)*R)*(RO*RO-R*R)
            DUI(I,J)=TI*(R*R-RO*RO)/2
         33 CONTINUE
      C
            CALL OUTPUT(NSP,DS,NRP,'LATERAL INTEGRAL OF DU/DS',25,DUI)
            CALL OUTPUT(NSP,DS,NRP,'LATERAL VELOCITY',16,V)
```

Figure 14. Program listing

```
      C
      C     CALCULATE SECOND APPROXIMATION TO DEPTH
      C
            DO 36 I=1,NSP
            T0=0.
            DEPC(I,1)=0
            DO 36 J=2,NRP
            R=(J-1)*DR+R0
            T1=(1./DEP1(I,J)*(-1)*(V(I,J)*P/(1.+U(I,J))**P/(1.+R*C(I))
           **DU)(I,J)))
            DEPC(I,J)=(T1+T0)/2 *DR+TPN1/7./R*DEPC(I,J-1)
      36    T0=T1
            NRP1=NRP-1
            DEPK=0.5*(DEP1(I,1)*DEPC(I,1)+DEP1(I,NRP)*DEPC(I,NRP))
            DO 36 J=2,NRP1
      36    DEPK=DEPK+DEP1(I,J)*DEPC(I,J)
            DEPK=(-1.)*DEPK/NRP1
            DEP1A=0.5*(DEP1(I,1)*DEP1(I,NRP))
            DO36 J=2,NRP1
      36    DEP1A=DEP1A+DEP1(I,J)
            DEP1A=DEP1A/NRP1
            DEPK=DEPK/DEP1A
            DEPK2=1.-DEP1A
            DO 37 J=1,NRP
      37    DEP2(I,J)=(DEP1(I,J)*(1.+DEPC(I,J)*DEPK)*DEPK2)*D
      34    CONTINUE
      C
            CALL OUTPUT(NSP,DS,NRP,'DEPTH CORRECTION',16,DEPC)
            CALL OUTPUT(NSP,DS,NRP,'DEP TOPOGRAPHY',14,DEP2)
      C
            STOP
            END
      C
      C
            SUBROUTINE OUTPUT(NSP,DS,NS1,TITLE,LT,VAR)
            IMPLICIT REAL*8 (A-H, O-Z)
            LOGICAL*1 TITLE(LT)
            DIMENSION VAR(101,21)
            WRITE(6,100)
     100    FORMAT('1',5X,'   CURVED CHANNEL  DEP TOPOGRAPHY OUTPUT'/)
            WRITE(6,101)(TITLE(I),I=1,LT)
     101    FORMAT(/5X,'S(M)  ',3X,60A1//)
            WRITE(6,105)
     105    FORMAT(10X)
            DO 10 I=1,NSP
            S=DS*(I-1)
            WRITE(6,102)S,(VAR(I,J),J=1,NS1)
     102    FORMAT(/1PD11.4/11X,11D11.4)
      10    CONTINUE
            RETURN
            END
End of file
```

Figure 14. Concluded

POOR

QUALITY

ORIGINAL